DETECTION OF OLIGOMERIC FORMS OF AMYLOID-BETA USING REFRACTIVE INDEX INTERFEROMETRIC FIBER-OPTIC SENSORS FUNCTIONALIZED WITH BIOTINYLATED PEPTIDES IN THE CONTEXT OF PROBE SIGNATURE APPROACH AND ITS POTENTIAL TO DIFFERENTIATE BETWEEN AMYLOID "STRAINS"

Lyubov Vassilets, Bachelor of Science

Thesis

Submitted in fulfillment of the requirements for the degree of a Master of Science in Biomedical Engineering

School of Engineering and Digital Sciences
Department of Chemical and Materials Engineering
Nazarbayev University

53 Kabanbay Batyr Avenue,
Nur-Sultan, Kazakhstan, 010000

Supervisors:

Lead Supervisor Name: Professor Daniele Tosi

Co-supervisor Name: Associate Professor Cevat Erisken

April 2025

Declaration

I hereby declare that this manuscript, entitled “Detection of oligomeric forms of amyloid-beta using refractive index interferometric fiber-optic sensors functionalized with biotinylated peptides in the context of probe signature approach and its potential to differentiate between amyloid ‘strains’” is the result of my work except for quotations and citations which have been duly acknowledged.

I also declare that, to the best of my knowledge and belief, it has not been previously or concurrently submitted, in whole or in part, for any other degree or diploma at Nazarbayev University or any other national or international institution.

Name: Lyubov Vassilets

Date: 17.04.25

Acknowledgements

I would like to express my deepest gratitude to all the people who made this work possible. I want to thank my supervisor and advisor for being always present and responsive to any concerns; other researchers in the laboratory who always could find time to guide or help in my process of learning, as well as during the work itself. I am also thankful to my family who always support me in all I do because they know how much it means to me.

Table of Contents

List of abbreviations

Aβ	Amyloid beta
AB	Antibody
ACH	Amyloid cascade hypothesis
AD	Alzheimer’s disease
AFM	Atomic Force microscopy
BRE	Biological recognition element
CSF	Cerebrospinal fluid
DI	Deionized
FTD	Frontotemporal dementia
NFT	Neurofibrillary tangles
OFS	Optical fiber sensor
PBS	Phosphate buffer saline
PD	Parkinson’s disease
PET	Positron emission tomography
RI	Refractive index
SDI	Semi-distributed interferometer
SMF	Single more fiber
SPR	Surface plasmon resonance

List of Figures and Tables

Abstract

The topic of the thesis is a possible new way of detection of Alzheimer's disease (AD) biomarkers for early and more precise diagnostics based on the recent advances in the study of "strains" of amyloid beta and utilization of peptides for functionalization of RI sensors instead of antibodies. The main goal is to make the sensor more economical and robust in application, as well as to enable additional modalities for further study going beyond the primary detection of the analyte (e.g. detection of concentration vs mere presence of the target using machine learning), with probe signature approach further enhancing these possibilities. Using peptides at the second stage of the work instead of antibodies as the biological recognition element (BRE) is a promising way to make sensors considerably cheaper in the context of diseases associated with peptide and/or protein aggregates. Nowadays, peptides are widely used in electrochemical biosensing, reports on their use in optical biosensing are present but mostly stem from surface plasmon resonance (SPR) measurements with very few covering interferometric detection of refractive index (RI) change. Also, investigation of possible detection of different "strains" bears promises for more precise diagnostics since there are so called mismatch cases where presence of the amyloid aggregates by itself does not lead to cognitive impairment. It is of paramount importance to be able to differentiate between such cases and focus on people who really need intervention without unnecessarily stigmatizing others.

Keywords: *Amyloid beta, aggregation, prions, peptides, interferometric fiber optic biosensors, antibodies, neurodegeneration*

CHAPTER 1- (INTRODUCTION)

1.1 Alzheimer's disease

Our society experiences an increase in life expectancy due to the high level of social and economic development, but at the same time, and as a direct consequence, the prevalence of age-related conditions is also on the rise. Neurodegenerative diseases (dementias) feature very prominently among them, bringing social, psychological and economic burden to many households worldwide. Alzheimer's disease (AD) is the most common cause of dramatic cognitive decline and is expected to affect around 113 million people by 2050 [1]. The problem is further complicated by the fact that in many countries, including Kazakhstan, there is not enough attention paid to this problem and population is largely unaware of it (personal communication with peers).

1.1.1 AD: discovery and pathology

In 1906 Alois Alzheimer discovered the two main hallmarks of the disease that nowadays bears his name, and they are still in the spotlight of scientific thought, that is Aβ plaques and neurofibrillary tangles (NFTs). The Amyloid cascade hypothesis (ACH) was established in the 1980s and still has a profound impact on the research and therapeutic options developed, although there is considerable criticism in its regard which cannot be ignored [2]. For example, there are reliably documented cases of "mismatches", that is people dying about the same age and with comparable burden of Aβ plaques, but one of them being diagnosed with Alzheimer's' disease before death, and another one cognitively normal [3].

Despite these doubts, amyloid beta aggregates and oligomers still constitute a valid diagnostic marker, although requiring a new way of interpretation and differentiation.

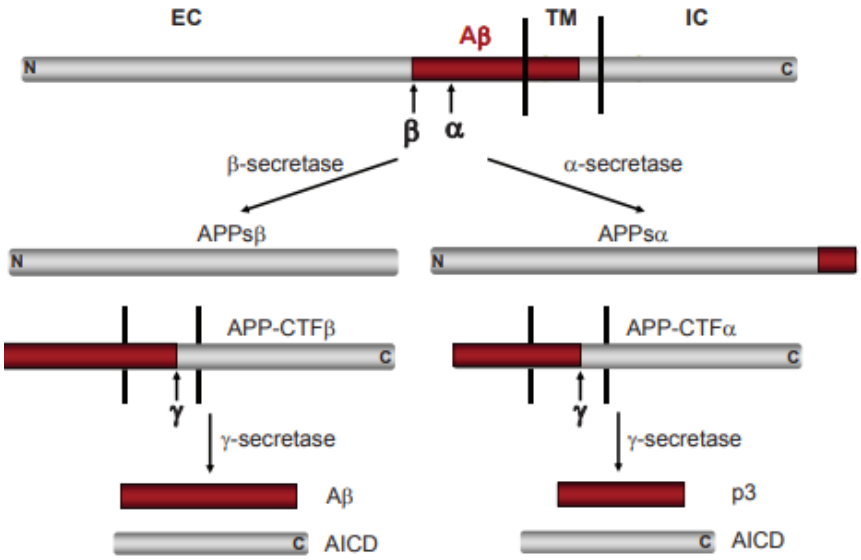

Figure 1: Schematic depiction of APP processing by secretases [4]

Figure 1 shows the pathway of processing of the amyloid precursor protein (APP), one of which leads to accumulation of amyloid beta peptides leading to their subsequent aggregation. APP is an important player in the nervous system since it localizes to the growing neurites near the forming synapses [4], its role in neurons is still not fully disentangled as well as the role of its multiple products. Its products include fragments cleaved from it by different proteases (including at least one caspase), including an AICD (intracellular domain) which although having only 47 residues has very important clusters and phosphorylation sites, acting as a transcription factor.

It is also important to mention that the current trend in early diagnostics is not so straightforward as we would like: Due to the mismatch between the amyloid burden and presence or absence of cognitive impairment the early diagnostics just by the fact of presence of amyloid oligomers in the CSF *per se* is a dubious criterion which can lead to stigmatization of people who might never develop AD in future. Therefore, it is crucial to suggest a new way in an attempt to overcome this problem.

The reasonable way is to hypothesize that there must be something besides the simple fact of the presence of the plaques and oligomers and their amount. In this work it is planned to investigate possibility to differentiate the underlying “strains” of protofibrils using fiber optic biosensors

detecting RI change upon the binding of the target.

Even before we can talk about strains *sensu stricto* it is essential to understand that there are different levels of Aβ aggregation. Different antibodies available now for detection or for treatment recognize only a certain range of the aggregated forms because an antibody is designed to recognize a certain epitope [5]. Fig. 2 below shows levels of Aβ fibrils organization, in the cited article Makowski [3] states that the strain identity is mostly preserved on the level of protofilaments because there is much more energy needed to rearrange them than higher order elements which can be much more varied and are not so valuable for strain identification. It means that the most important part, a "fingerprint", is the cross-β structure.

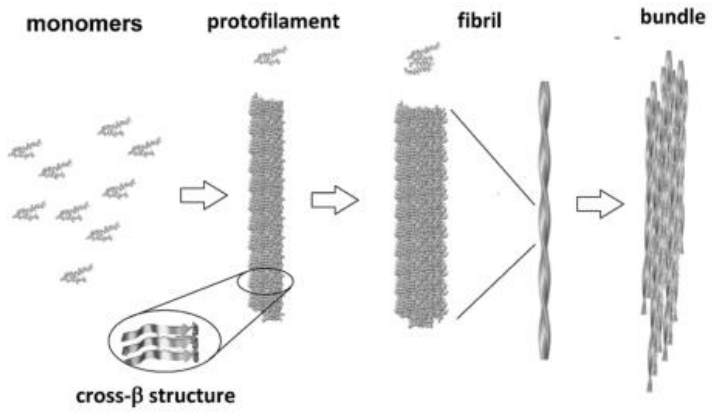

Figure 2: Levels of organization of amyloid beta peptide. Adapted from [3]

Postmortem studies give the picture of macroscopic appearance of the aggregates eventually formed by the fibrils pictured above (Fig. 2). It is mostly at this stage when we generally can study different strain composition of aggregates nowadays which is already too late.

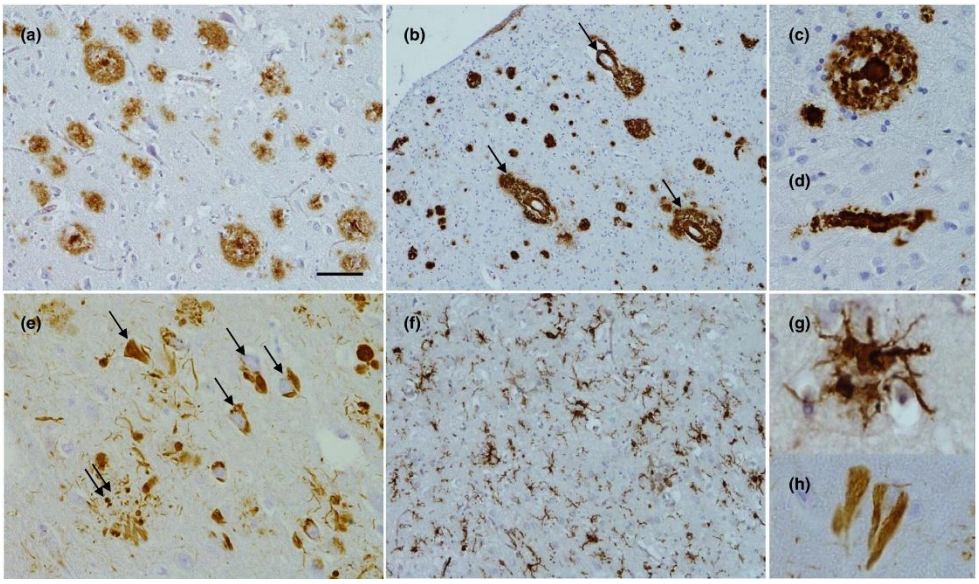

Figure 3: Pathology of Alzheimer's disease. Amyloid beta immunohistochemistry postmortem.

Adapted from [6]

Figure 3 shows tissue slides obtained from patients after they died, it is clearly seen that even on this level the aggregates appear different. The character of prions however gives hope to study aggregates after their extraction from a living patient.

1.1.2 Symptoms

The huge societal and economic burden caused by AD is due to the fact that it primarily affects the cognitive functions of the patients, so they not only drop out of the productive life but also cannot handle routine tasks which causes additional costs for the care as well as psychological impact influencing their families interfering with their performance as well. Figure 4 gives an overview of the AD symptoms as they progress.

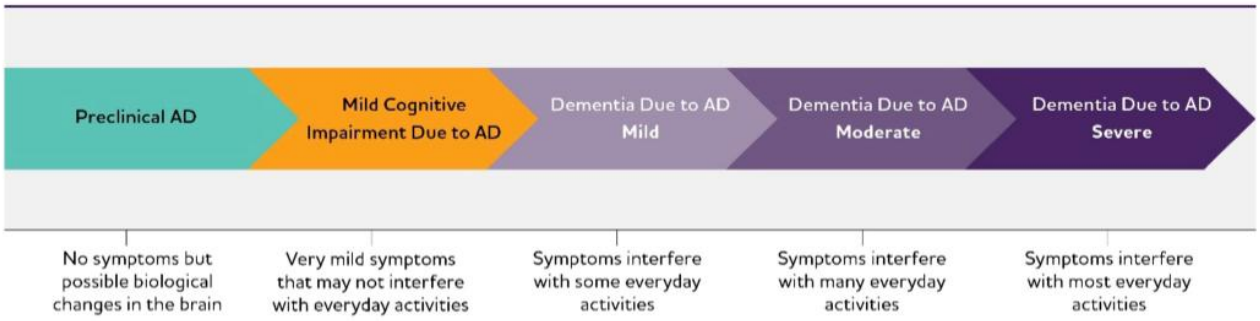

Figure 4: Course of symptoms exacerbation throughout the disease progression. Adapted from [7]

1.1.3 Importance of early diagnosis

As of today, there is no cure for AD therefore the early diagnosis is of vital importance: it can help to modify some risk factors possibly allowing to slow the progression of the disease. At the same time, early diagnostics can be stigmatizing. It is important to understand that just presence of amyloid beta aggregates is not a sure sign of dementia in future (see mismatch cases mentioned above) therefore we should not only find a target aggregate but also differentiate between its possible variants which can be conductive to very different outcomes. The possibility to do so even on the stage of biosensors is important, since biosensors operate using small sample volume but for traditional ways of structure determination greater volumes are usually needed as well as previous modifications (for

example in NMR), whereas in the case of the RI biosensors even labeling is not needed. This task is challenging therefore the main emphasis of this work is on providing a proof-of-concept study using markedly greater concentrations than those found physiologically with the perspective of that if the results are positive the same procedure can be subsequently adapted to the physiological range with appropriate improvement of the sensitivity.

1.1.4 Main pathological signs: amyloid beta

As it was described in Keep et al. (2023), amyloid cascade hypothesis despite growing number of objections is still reigning supreme in large-scale paradigm of drug development [2]. Even if eventually, it is proven wrong amyloid beta will remain a valid diagnostic marker worth considering. Now attention is growing in regards to different strains of misfolded proteins and peptides. It was proven that in case of another devastating neurodegenerative disease, Parkinson's disease, which is also connected to protein aggregates (alpha-synuclein), there are different types ("strains") of aggregates with disparate characteristics [8]. The same process is happening in case of amyloid beta: aggregates of amyloid beta are known to have different structure despite the common underlying sequence [3]. On the Fig. 5 below you can see a pictorial representation of fibrils and microphotographs of aggregates existing.

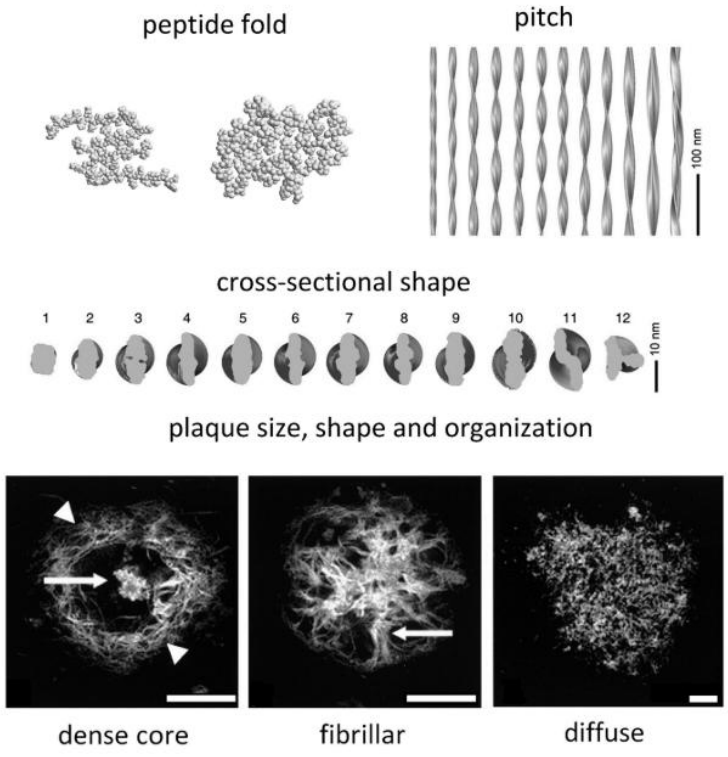

Figure 5: Fibrils and aggregates. Adopted from [3]

Despite extensive study about the harmful aspects of amyloid beta the primary physiological role of

APP is often overlooked. However, to conduct proper research we have to consider everything. There is a hypothesis that contribution of the APP to the development of AD can be also related to the loss of function not only to gain of toxic function in case of the amyloid beta fibrils and aggregates. Yet unfortunately, “By comparison, whether full-length APP or other non-Ab APP processing products play a significant role in AD or contribute to other neurological disorders has received somewhat less consideration” [4]. In this work we also focused on amyloid beta peptide over other cleavage products, yet keeping in mind their potential implications.

Fortunately, now the understanding is growing that structural features matter a lot: “In contrast to globular proteins, a single protein sequence can aggregate into several distinctly different amyloid structures, termed polymorphs, and a given polymorph can reproduce itself by seeding. Amyloid polymorphs may be the molecular basis of prion strains.” [9]. With that diagnostic techniques are also bound to be enhanced.

There is lot of research work dedicated to the strains of amyloid beta aggregates, “Evidence is building for the idea that clinicopathologic heterogeneity observed in AD patients may arise from distinct structural variants, or strains, of the causative misfolded proteins”[10]. Of course, the possibility that the main reason for pathology is a loss-of-function of APP should never be discarded completely until proven. APP is an extremely versatile protein which is implicated in many vital cellular events and undergoes extensive posttranslational modification, harbors important motives and is cleaved in several parts each with a separate set of functions [11]. Amyloid beta is implicated in the development of yet another key pathological AD sign – NFTs, which are addressed in the next sections. As of today, there is no clear picture of exactly how amyloid plaques or oligomers which presumably start to form in endosomes and then are expelled from the cell and accumulate in the extracellular region can affect the formation of NFTs which are strictly intracellular. There is a hypothesis that the interaction between amyloid plaques and membrane is involved but there is also

a possibility that some other cleaved fragment of APP can potentially be involved in NFT formation quite apart, although parallel to extracellular amyloid aggregates.

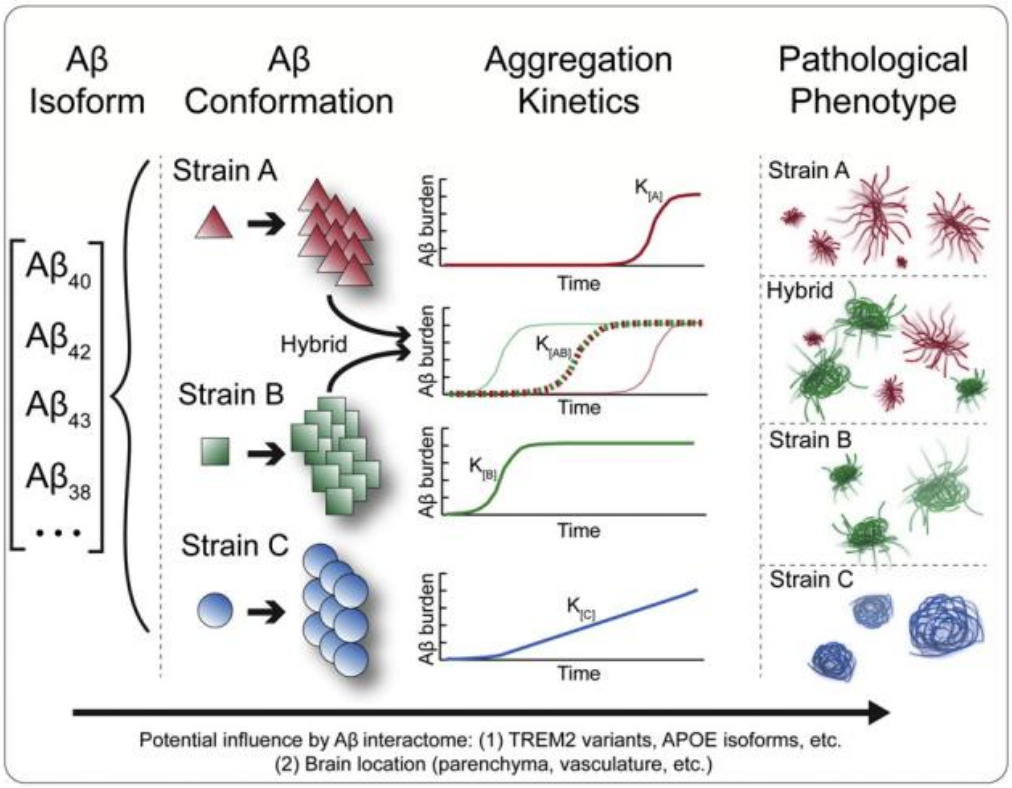

Figure 6: Adapted from Condello et al. (2018) [10]

Figure 6 presents amyloid strains formed under different conditions within the organism while interacting with varied proteins and other biomolecules. The differences can be great. *In vitro* it is hard to reproduce intracellular or extracellular milieu therefore for our proof of concept we took non-physiological but clearly different conditions which are easily reproducible in the laboratory.

Currently there are few efforts to use biosensors to differentiate between the strains directly during the diagnostic procedure, therefore such question seems to be justified.

1.1.5 Main pathological signs: NFT

Alongside amyloid beta aggregates microtubule-interacting protein tau is another main pathological sign noticed originally by Aloise Alzheimer in 1906. Unlike amyloid beta aggregates where we still

cannot pinpoint the exact mechanism of toxicity, it is much more understandable in case of tau: its disfunction directly leads to microtubule disorganization. The axons of neurons depend heavily on the intact structure of microtubules, so it is clear that any defect in microtubules will lead to devastating consequences.

1.1.6 Prion nature

There is a parallel traced by multiple researchers between AD and so-called prion diseases. Prions became some sort of revelation to the scientific community introducing protein as an absolutely novel infectious agent. Stanley B. Prusiner made this revolutionary discovery in 1982 [12]. According to data available AD can be viewed as a type of prion disease therefore it is important to assess how this analogy can affect diagnostic methods. Characteristic of prions includes presence of different "strains" which can cause very different effects [13].

It is significant that different strains are implicated in yet another neurodegenerative disease in the case of aggregate-forming protein TDP-43, which is the cause of fronto-temporal dementia (FTD), and also features in several pathologies more [14].

One of the salient characteristics of prions, which is as well observed in amyloid beta, is how readily a single monomer (in this case peptides, not separate amino acids) gets incorporated into oligomers. On these facts rests the second part of the current work: using peptides as substitution for ABs.

This statement is made even more justified by the suggested mechanism of transmission of AD in humans, where several cases of disease developed after grafting tissues from an affected person to a patient with different condition (trauma, for example) or given cadaveric growth hormone to an otherwise healthy individual [15].

1.2 Diagnostics of AD

It is extremely important to diagnose the disease in time. In the case of neurodegenerative diseases, it is especially hard because symptoms can be confusing and misleading at first. For example, PD pathology can be most prominently seen on the postmortem slices of brain tissue, it is hard to image during life of a patient. In the case of AD the problem is exacerbated by the fact that changes in the brain which can be visualized appear decades after the disease began to unfold, already at the symptomatic stages, thus delaying any possible measures.

1.2.1 Gold standard: PET

Positron emission tomography (PET) at the present is the most widely used modality for diagnosis of AD [16]. But as was mentioned before it shows signs of the disease when it has already gone too far for any modifying strategy to make a considerable difference. Also, there is another drawback, "Current amyloid PET imaging agents (i.e. PiB, Flutemetamol, etc.) based on the Thioflavin T scaffold may only detect a specific Aβ conformational strain" [10]. That is this imaging can potentially miss out on pathological strains, even big deposits of aggregates which do not bind these dyes.

It was documented that "a subset of patients (bearing hypothetical Strain A) exhibit AD symptoms and fluid biomarkers *antemortem* and abundant neuropathology *postmortem*, but can test negative for amyloid PET signal"[10].

1.2.2 Markers for AD

There is a whole spectrum of markers which can be used to diagnose AD [17]. For these different bodily fluids are used, there are attempts to measure certain biomarkers even in adipose tissue [18].

The pathological signs mentioned above (amyloid-beta and NFTs) are used as the major biomarkers. The greatest concentration of them, apart from the brain itself, is observed in cerebrospinal fluid, with much lower abundance in blood. Since the current work is a proof-of-concept study we used PBS instead of CSF in order to simplify the first stage of investigation with perspective to use artificial CSF on the next stage and real CSF from patients on the final stage (PhD).

The feasibility of using peptides for the study is underlined by the fact that in AD pathology there are different types of amyloid beta involved, not only amyloid beta 42 and 40 [19]. Studying only pure peptides is highly idealistic and poorly reflects reality since “In vivo, the sequential cleavage of the amyloid precursor protein results in the cooccurrence of multiple variants in the brain’.[19]

1.2.3 Biosensors

Biosensors present a blooming field which can help in early diagnostics of AD, electrochemical biosensors and SPR biosensors are the most used by far nowadays [20]. Nevertheless, interferometric optical biosensors based on the change in refractive index are also promising and present a wide field of opportunities.

In the case of this work OFS based on special type of optical fiber is used. Due to its unique characteristics described in the original article by Kaziyev et al. (2023) and highlighted in the sections below it allows to apply different approaches all based on the well-known practice of functionalization of glass surfaces since optical fiber is essentially glass (silica with additives).

1.2.4 Refractive index interferometric fiber optic biosensors

For this work refractive index fiber optic biosensors were used and here a description of them is provided. The sensors used in this work are the result of cooperation between several labs. While

their properties are unique, we can classify them as interferometric inline fiber optic sensors working on the basis of Fabry-Perot principle, that is “composed of two parallel reflecting surfaces separated by a certain distance” [21]. This article describes sensors in general terms, as to the particular sensors we used in this work the Fabry-Perot structures were created by incorporation of magnesium nanoparticles into the fiber core. The creators of this sensor published an article dealing specifically with the sensors used [22]. It contains all the details of the work principle and gives insights to the fabrication process.

One more advantage of the used interferometric biosensor is a low biofouling of glass, whereas electrochemical sensors’ electrodes are “prone to strong biofouling when exposed to biological fluids” [23].

1.2.5 Peptides used for sensing: comparison

There are multiple examples of using peptides as biological recognition elements but mostly in the case of electrochemical and SPR sensors which makes investigations of interferometric RI sensors all the more interesting.

Table 1 below provides a brief overview of several sensors utilizing peptides as recognition elements, including sensors used in the current work.

Sensor	Detection mechanism	Functionalized substrate	Biological recognition element	Target	Limit of detection	Grafting of BRE	Ref.
Fiber optic semi distributed interferometric refractive index biosensor	RI change	Optic fiber	Biotinylated pegylated peptide (Abeta 42)	Aβ 42 (oligomers, all sizes of aggregates)	To be found in future work	Aligned (supposed to be, due to biotin)	This work
Optical nanosensor for intracellular and intracranial detection	Solvatochromic modulation of the near-infrared emission of the nanotube	Single walled carbon nanotubes	Amyloid beta 42 peptide, monomers	Aβ 42 (oligomers, all sizes of aggregates)	100 nM in PBS	Stochastic	[24]
Electrochemical sensing platform based on gold nanostars	Impedance changes	Gold nanostars (AuS)	Prion protein-peptide probe, PrP^c	$A\beta_o$ oligomer	2 pM	Stochastic	[25]
Electrochemical biosensor using a microporous gold nanostructure	Differential pulse voltammetry	Gold nanostructure	Amyloid beta 42 peptide	Aβ 42 (oligomers, all sizes of aggregates)	0.2 pg/mL	Stochastic	[26]
Label-free SPR for serum analysis	SPRi	gold-coated glass chip	ADP3 peptoid	Aβ 42 (oligomers, all sizes of aggregates)	NA	Stochastic	[27]

Table 1. Variants of using peptides as BRE

1.3 Software

For this work MATLAB and Python programming languages were used.

There are several scripts employed at different stages of the work, first of all scripts for calibration, data loading and data analysis (you can find all scripts using link provide).

Calibration is a necessary step which gives crucial information about the quality of the sensor. Due to inherent stochasticity of the fabricated sensors, as described in Kazhiyev et al. (2023), the sensitivity levels as well as the number of peaks and valleys can vary significantly. There is a suggestion to use calibration data to create a probe signature and include it as an indispensable part of the whole probe. Such signature will be used consequently to provide more data points for analysis together with measurements in the blank solution.

Data analysis is a crucial step since the sensors used are not the commonly applied ones and the protocols for their handling are being developed in our laboratory by other researchers. After the creation of a probe signature, it potentially can be possible to characterize the pattern of binding more clearly since during calibration the refractive index changes smoothly all over the sensing surface, but in the case of the target binding the changes can be patchy which is supposedly reflects on the results.

The idea is to create a model of the sensor on each step of its functioning starting with the general considerations such as the diameter of the fiber and of the core since the cleaved core is the region where sensing happens. The physical characteristics of the fiber are extensively explored in the original article by Kazhiyev et al. (2023). The question remains as to whether the sensitivity is given by microparticles inside the core or just on the surface of it, that is exposed in the process of cleavage and subsequent chemical treatment of the fiber.

Another possibility is to use machine learning for data analysis in order to extract information about concentrations of the binding target. The number of sensors used is limited to 4-5 per detection but

each of the sensors has several spectral features which have different levels of sensitivity, each of these features can potentially be used as a separate “sensor” in the context of data analysis. The volume of data is feasible to analyze using open-source software and standard Python machine learning libraries, such as sklearn.

Training data will include data from detection using known concentrations of the target, another part of the detection data will be used for validation. Experimental data are produced by measuring “unknown” concentrations, that is concentrations not disclosed in the code directly but known to the investigator; this way it is planned to assess ability of the sensors to give information about the concentration of the target analyte, not just its presence because in the case of amyloid beta simple presence of the aggregates or oligomers in the sample does not represent diagnostically definitive information.

As was mentioned before, the probe has stochastic nature which becomes even more stochastic upon functionalization since there is no way to control the placement of the BRE on the probe (on the first stage it is ABs, on the second stage – peptides). It is hypothesized that peptides can give a better signal since streptavidin used before grafting the biotinylated peptides is three times smaller than an average antibody (50 kDa vs 150 kDa) thus potentially giving 3 times increase in grafting density, therefore more binding sites available for the target to attach itself.

1.4. Framework of the Study

The work was initially divided into two stages due to the availability of the reagents. Nevertheless, this allowed us to make the work more comprehensive and supplied data for comparison.

The first stage is dedicated to testing the hypothesis of detecting different “strains” using an already validated method – detection of the target molecule using ABs. On the downside of the antibodies is

the fact that they are sensitive to a specific epitope which might not be present in all targets due to different reasons: mutation, inadvertent posttranslational modification, interaction with therapeutic agents, etc. Even so, the antibodies are a gold standard for detection of the targets in biological samples due to their high affinity and specificity, as well as thoroughly developed protocols for their production and implementation. Monoclonal antibodies are also used extensively as a specific therapeutic modality; therefore, we can say that the same principle governs their utility in both spheres of diagnosis and treatment.

The first stage includes attempts to differentiate based on the sensor response between the target molecules aggregated under different conditions. This is the proof-of-concept step therefore conditions chosen were markedly different:

- Stock solution diluted in the standard PBS and used immediately after the dilution;
- Sample aggregated in the standard PBS solution for 12-15 hours under ambient conditions at concentration higher than critical aggregation concentration (90 nM in case of amyloid beta 42 [28]);
- Sample aggregated in the PBS solution diluted with DI water (2X) and incubated for 16-18 hours under ambient conditions at the same concentration as the second sample.

For detection of each variant 4-5 sensors were used (the limitation due to the number of available channels of the optical detection system). The peculiarity of the SDI sensors used is in the fact that each sensor (from the four-five mentioned) gives several readouts which can be analyzed separately or jointly, thus supplying more data points. This brings additional opportunities from the point of view of statistical analysis as well as the complexity we are currently dealing with.

As one of the possible future steps it is also suggested to use disaggregation analysis. It will be perfect

for the RI sensor in case of amyloid aggregates since unlike the usual targets (proteins) the aggregates are characterized also by kinetics of disaggregation. For this purpose certain chemicals can be used like in an article describing chemical clearance of amyloid deposits [29]. This chemical can be promising not only as a therapeutic one but also as a basis for additional diagnostic modality. There is another article describing possible biophysical mechanisms of action of EPPS and proposing that this compound can be promising also for PD (Parkinson's disease) [30].

There is also a possibility (possible to explore on PhD level) to combine RI measurements with other modalities due to the highly unreactive characteristics of the probe itself (silica) which are unlikely to negatively affect other measurements. For example, dyes are frequently used to assess amyloid beta aggregation, in a recent article authors report a probe which they call "the only probe capable of detecting significant differences across all oligomeric species of β-amyloid" pTP-TFE [31].

CHAPTER 2 - (MATERIALS AND METHODS)

In this part there is information on the following: i) materials and equipment used, ii) principle of the sensor used, iii) functionalization protocol, iv) sample preparation, v) detection, and vi) data analysis.

2.1 Materials

As was mentioned above, the work is divided into two stages. At the first stage, readily available reagents were used which are listed in the table 1 below.

Name	Manufacturer	Catalogue number
Recombinant Anti-Alpha-synuclein (phospho S129) antibody [EP1536Y]	Abcam	ab51253
Recombinant Anti-beta Amyloid 1-42 antibody [mOC64]	Abcam	ab201060
Alpha-synuclein (phospho S129) peptide	Abcam	ab188826
beta-Amyloid Peptide (1-42) (human)	Abcam	ab120301
Human Amyloid Beta 42 ELISA Kit	Abcam	ab289832
Alpha Synuclein Phospho-Ser129 (SNCA pS129) Cell ELISA Kit	Abbexa	abx596009

Table 2: Reagents for the first stage of the experiment

For the next stage of the work the reagents are listed in Table 2 below.

Name	Manufacturer	Catalogue number
1,1,1,3,3,3-Hexafluoro-2-propanol	Meryer	M29682-25G
Thioflavin T	Meryer	M64470-1G
Biotin	Meryer	M74859-5G
Biotin+PEG+Ab 40	Pepmic Co Ltd.	NA: Custom made
Biotin+PEG+Biotin Ab 42	Pepmic Co Ltd.	NA: Custom made

Table 3: Reagents for the second stage of the experiment

All chemicals were acquired from several manufacturers: Abcam, Abbexa, Meryer, Pepmic (custom synthesized peptides). Streptavidin was kindly provided by fellow researchers from another lab,

already in reconstituted form, after which is was aliquoted and kept in the refrigerator at 17-20° C. The justification to use peptides as a substitute for ABs in the second stage of the experiment is the fact that their binding to aggregates has been already proven [24] and they are much cheaper to produce than antibodies. Also due to the presence of biotin on one end they can be immobilized in an oriented manner as opposed to the most examples of peptide use, as well as antibodies, which according to the current protocol attach to the probe in stochastic orientations. Antman-Passig et al. (2022) have proven that amyloid oligomers can bind amyloid beta peptides absorbed at the surface of carbon nanotubes, that is having very distorted and irregular configurations, it was assumed that binding can be even more efficient if the peptide is in a more relaxed configuration: functionalized on the surface of the probe using biotin-streptavidin interaction and a linker to guarantee more space.

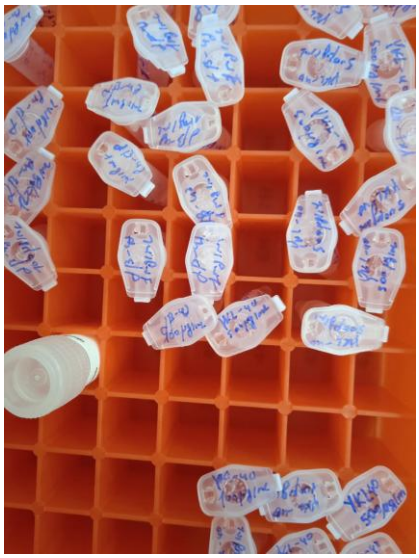

Figure 7: Reconstituted peptides and ABs for analysis.

2.2 Fabrication of the optic fiber probe

The principles of SDI sensor work were exhaustively described in Kazhiyev et al. (2023) [22], the fabrication steps were also described therein.

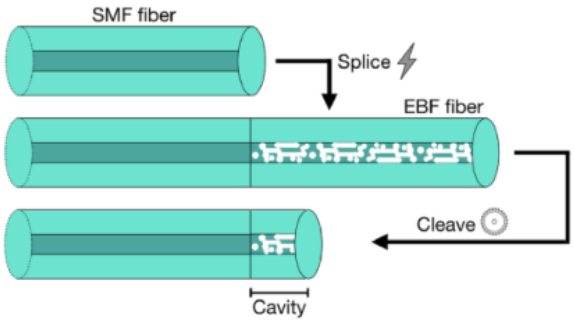

Figure 8: The SDI sensor. Adapted from the original article [22]

The first step requires fabrication of sensors which consists in splicing special types of fiber with magnesium oxide-based nanoparticles (also known as “Wilfred fibers”) to a usual SMF fiber, thus SMF forms the basis of the sensor while the final stretch of the special fiber is a sensing element (see Fig.6).

The important part of the work is that all the steps from fabrication to data analysis are made by the author. This process takes time but shows that eventual commercialization can benefit from an economically feasible scheme making sensors more affordable. Figure 7 below shows one of the steps, splicing of the fibers.

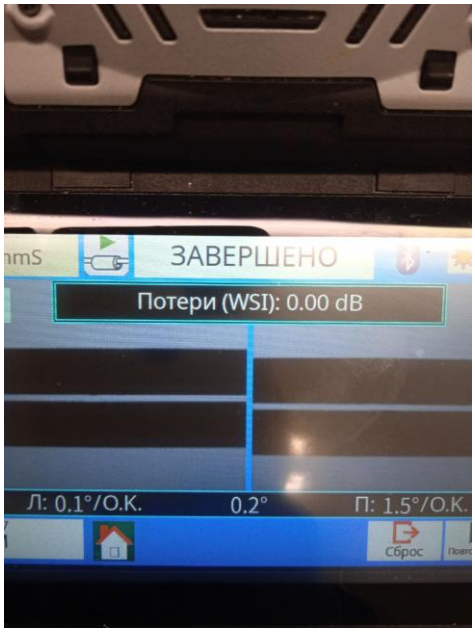

Figure 9: Splicing of fibers. Here SMF fiber is already spliced to the “Wilfred fiber” and ready to

be cut, after cutting the sensor is ready for functionalization.

2.3 Functionalization of the optic fiber probe

The functionalization of the probe *during the first stage of the experiment* was carried out using a validated protocol which is routinely used in the Biosensors and Bioinstrumentation laboratory.

The sensor itself is made of glass (silica) that is why the protocol of functionalization is already very profoundly studied and validated.

The first step of functionalization is treatment of fiber with “piranha” solution. This acidic solution removes organic residues from the fiber and enriches the surface with functional groups (hydroxyl, -OH) which are necessary for the consequent steps.

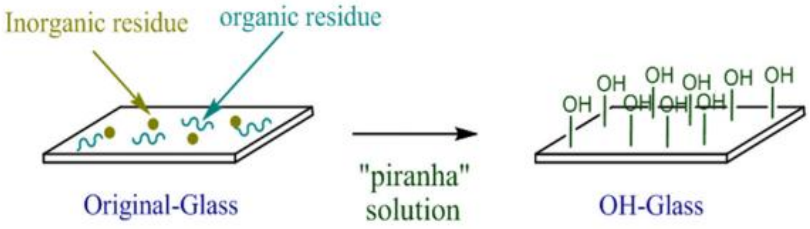

Figure 10: Glass surface after the piranha solution. Adapted from [32]

The piranha solution is prepared under fume hood where sulfuric acid (H2SO4, 98%) is added to hydrogen peroxide (H2O2, 30%) in proportion 4:1 in a glass vial. During this process all necessary individual protective equipment (lab-coat, gloves, googles) is used. After incubating in piranha solution for 20 minutes sensors are rinsed with DI water and dried using N2 gas.

The second step is silanization: immersion of fibers in APTMS (3-aminopropyl)trimetoxysilane) diluted in methanol for 15 minutes. The ratio is 14.85 ml of methanol:0.150 mL APTMS. After that the fibers should be washed with methanol and dried properly.

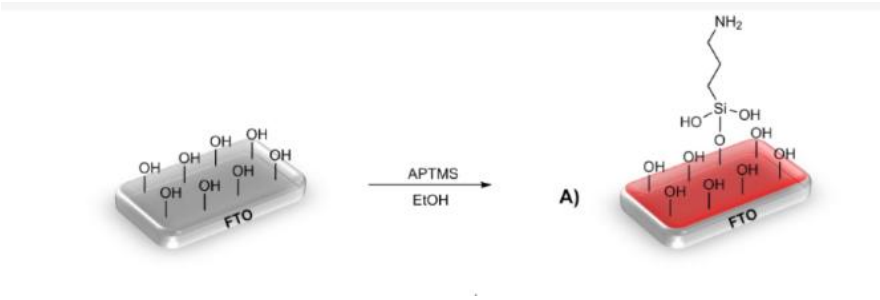

Figure 11: Silanization process using APTMS. Adapted from [33]

During the next step fibers are placed in the oven in a special glass beaker and kept at 110°C for 1 hour. After the baking step fibers are rinsed with DI water.

Further fibers are incubated in 1:1 solution of glutaraldehyde (GA) in phosphate buffer saline (PBS) (500 µL of GA and 500 µL of PBS) for 1 hour.

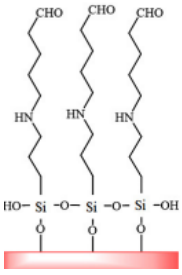

Figure 12: Fiber surface after GA treatment. Adapted from [34]

Then fibers are rinsed with PBS and are ready for the next step, that is functionalization of interferometric biosensors with the antibodies to measure the content of the biomarker.

At this step of the thesis work usual antibodies against the target biomolecule are utilized: antibodies against amyloid beta (done) and alpha synuclein (in progress). Molecular weight of an antibody is usually 150 kDa.

Antibodies attach to the surface of the probe using amino groups: it can be an amino group on N-terminus, as well as a lysine, therefore the process can be stochastic.

Before functionalization target antibodies are diluted in PBS to the needed concentration. Prepared

fibers are then incubated in the produced solution for 1 hour.

The next step is blocking the remaining functional groups to avoid possible interference during sensing. In this case 10% m-PEG is used as an effective blocking agent.

The usual volume of preparation is 50 μL mPEG solution (0.05 g m-PEG in 500 μL PBS). The fibers are incubated for 30 minutes. Then they are rinsed in PBS and stored in a tube filled with fresh PBS till their utilization for detection.

The second stage of the experiment included utilization of biotinylated peptides with PEG linker as BRE instead of the antibodies. There are different protocols for the functionalization of sensors with peptides but in most cases such protocols concern electrochemical or SPR sensors which have different surface chemistry as compared to the optical fiber used in our RI sensors. Therefore, it was decided to modify the existing protocol which has already been proven valid by the addition of two steps. All the steps described above are followed but instead of antibody streptavidin (4 μL/mL, the same as antibodies) is used, after last step of the previous protocol (blocking with m-PEG), there are two more added:

1. incubation with biotinylated peptides (1 hour), concentration 4 μL/mL, and
2. blocking with free biotin to prevent unspecific binding (30 minutes), amount of biotin was chosen 0.05 g per 500 uL of PBS (by analogy with the previous blocking agent, m-PEG), but then reduced to 0.01 due to the solubility issue.

The general functionalization protocol of Stage I (step by step):

1. Piranha-solution pre-treatment: 4:1 v/v H2SO4:H2O2, incubate for 15 minutes in the hood;
2. Rinse with DI water, dry using N_2;
3. Sialinization: 14.85 mL methanol + 0.150 mL APTMS, incubate 20 minutes;
4. Wash with methanol and dry;

5. Heating at 100°C in the oven, 60 minutes;
6. Crosslinking step: immerse in 1:1 solution of glutaraldehyde (GA) and PBS (500 μL GA + 500 μL PBS;
7. Rinse with PBS;
8. Incubate with the target antibody (here ABs against Amyloid beta 42), 4 μg/mL (here 4.7 μL of the AB stock + 995.28 μL PBS);
9. Blocking using m-PEG (here 0.05 g m-PEG + 500 μL PBS);
10. Rinse with PBS, and
11. store in a tube with PBS until utilization.

The general functionalization protocol of Stage II:

1. Steps 1-7 from the Stage II protocol;
2. Incubate with streptavidin (4 μg/ml), 60 minutes, PBS;
3. Blocking using m-PEG (0.05 g m-PEG + 500 μL PBS)
4. Incubate with biotinylated peptides (4 μg/mL), 60 minutes;
5. Blocking using biotin (0.01 g/mL) 30 minutes;
6. Rinse with PBS, and
7. Store in a tube with PBS until utilization.

2.4 Sample preparation

The goal of the work is to see whether different states of aggregation influence the features of detection. Therefore, for detection several variants of samples are used:

- traditional sample: stock solution is taken as it is from the fridge where it is kept in accordance with the IFU supplied by the manufacturer, then it is diluted to the necessary concentrations with PBS. After that detection follows immediately;
- incubation overnight sample: stock is taken and diluted with PBS to the critical concentration of aggregation (e.g. 90 nM/mL in case of amyloid beta [28]), then it is incubated under ambient conditions for 12-14 hours (after this time the solution becomes turbid which is the sign of aggregation);
- incubation overnight using modified PBS (in this case diluted 2X PBS) to ensure incubation is performed under different conditions.

The conditions are markedly different because the current work is proof-of-concept and samples very different from each other are needed. If there is a confirmed and reproducible difference in detection, then the next run of the experiment will probe more subtle differences.

During the second stage of the experiment the sample preparation proceeds according to the same protocol to ensure comparability.

2.5 Detection of the target

Micronoptics analyzer (see Figure 13) with 5 working channels and laser light source is used to perform calibration and detection of the samples. Probes are connected to special connectors using so-called “pigtails”.

Figure 13: Optical analyzer MicronOptics

During measurement the data is collected using ENlight software which allows to detect change in the refractive index caused by binding of analyte to the receptor (antibody) (http://micronoptics.ru/tutorials.html).

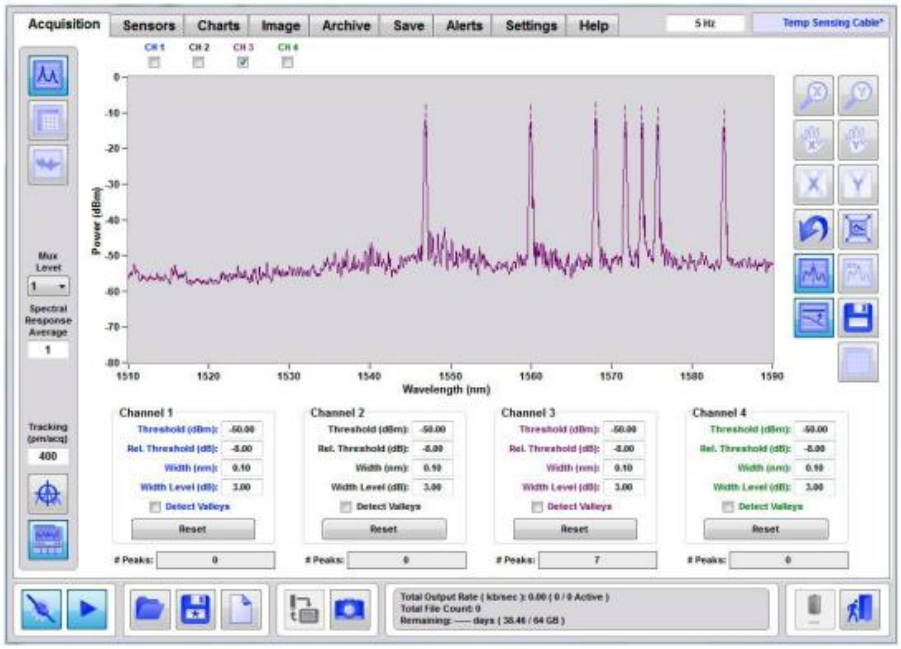

Figure 14: Example screen showing data acquisition process. Adapted from [35]

At the moment calibration step is used to assess if the probes have sensitivity, but there is an idea to use calibration to create “probe signature”. This potentially can help in analyzing detection data by providing information on the probe behavior in the case of monotonous RI change (in sucrose

solution). The hypothesis is that in the case of the target binding the change of the RI is not homogenous and this can provide additional information about the sample, possibly giving opportunity to differentiate between concentrations. For this purpose, it is planned to create a Python script which can be eventually applied to other sensors too in case it shows significant results on the later stages of the work (possibly PhD).

After the detection step data analysis is performed using specially developed MATLAB scripts.

The new scripts for comparing runs using different samples are under development.

2.6 Data analysis

The lab has an established data processing routine but in case of this experiment there is need to modification of the existing scripts and compiling a new one. The work is carried out in collaboration with other lab members who are more experienced in coding.

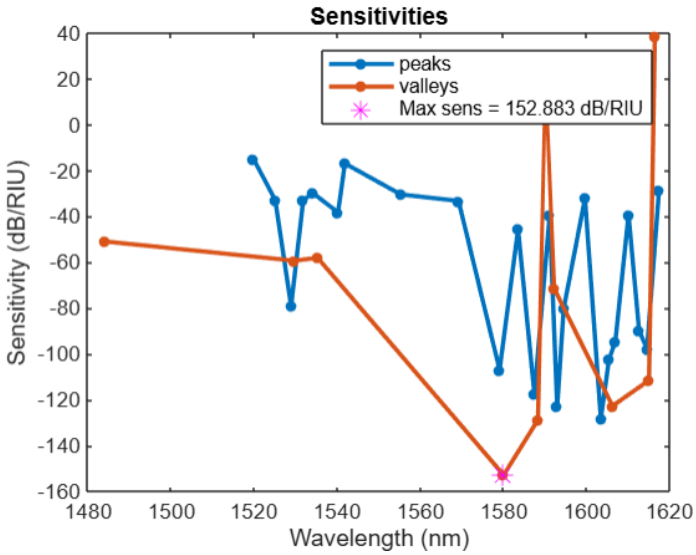

Figure 15: Evaluation of a probe sensitivity after calibration (an example from the current work).

Figure 15 above shows the peculiarity of the SDI sensors, that is the presence of multiple peaks and valleys sensitive to the RI change. While for each sample only five sensors were utilized, each of

them had at least several peaks or valleys which can be analyzed jointly or separately thus giving an additional dimension to the data analysis, although also contributing to its increased complexity.

There is no commercially available software to perform data analysis task therefore the new solutions are being investigated, among them possibility to use calibration data for creation of a probe "signature". The idea is to find sensitive peaks and valleys, mark their positions and sensitivities and use this data during the next step. This will require creating a probe-tracking protocol to make sure that the signature is associated with the right probe. The suggestion is to create a unique code name for a probe to guarantee its tracking throughout the process. The name will be incorporated in the general data analysis pipeline to eliminate possibility of confusion. Currently, the suggested protocol is as follows:

- Upon verification that the probe works (spectral signal on the screen) each probe is supplied with the code name constructed in the following way: type of the fiber used – date (in format DDMMYY) – initials of the owner - code name of the probe (or number given by the owner), guaranteeing the unique ID, for example: SP4_300125_LV_LV2;
- This data should be added to the reference file .txt;
- After calibration is completed the data analysis follows which determines which probes have acceptable sensitivity;
- The part should be added to the Python script in order to save the probe signature and store in in the .csv format, there will be a separate file for each probe because not all probes have acceptable sensitivity and some can be discarded from the batch;
- After the detection and routine data analysis the probe signature file can be used to run additional analysis or/and machine learning to infer detected RI based on the calibration data which potentially can help in defining the concentration of the target.

2.7 The second stage of the experiment

After the antibody stage is finished, peptides are used as BRE. The plan is to follow a similar procedure with necessary modifications due to the change of the BRE and to compare the results thus gaining more robust understanding of the advantages or limitations of the method proposed.

The peptides were custom synthesized by Pepmic and received on January 31, 2025 thus marking the beginning of the second step of the work. The peptides are provided in powder form and needed to be reconstituted. Peptides were shipped at ambient temperature, and are highly stable at lyophilized form in sealed bags. Upon receipt, lyophilized powder was stored at -20°C or lower (for long term storage (3months +) a -80°C freezer should be used). Reconstituted peptide was aliquoted into several freezer vials and stored at -20°C or lower, subsequently it is necessary to avoid freeze-thaw.

The peptides were reconstituted using appropriate buffer (PBS) and aliquoted for subsequent experiments. The procedure was the following: first, the tube with peptides was centrifuged to ensure all the product was at the bottom of the tube and nothing was lost during opening. Then 1,3 mg of Amyloid beta 42 peptide were taken to be reconstituted. For reconstitution standard PBS solution was used, after adding PBS to peptides they were left to dissolve for 30 minutes. Half of the peptides appeared not dissolved at the end of this time interval, therefore it was decided to leave the tube with peptides in the -4° C freezer overnight. The next day inspection showed that there was still some amount of peptides which was not dissolved. To assist dissolution 50 μL of ammonium hydroxide were added and the mixture left for another 15 minutes to dissolve. After this step, the dissolution still was not complete, therefore it was decided to add 50 μL of DMSO solution, after that the remaining amount of peptides dissolved quickly within a minute. After that the dissolved peptides were aliquoted in the marked tubes and placed in fridge for storage before further use.

Due to the small size of the peptides it is unlikely that AFM will show their presence on the probe, instead AFM can show the presence of streptavidin which is much bigger. Given the character of the interaction between the biotin and streptavidin it is assumed that once streptavidin bound the peptides will bind to it trough biotin. Therefore, the efficiency of functionalization will be probed by response during detection. It is planned to perform three runs in order to find the best protocol, this number was chosen due to the time limitations of the current work with the perspective to carry additional runs on the level of PhD work to optimize sensitivity.

2.8 AFM imaging

Functionalization using antibodies is an established process but in the case of peptides there will be carried out additional imaging using atomic force microscope (AFM) in order to guarantee that the chosen way of functionalization is valid for peptides on the later stages of the research due to time limitations.

As a preliminary stage the imaging of the fiber was already carried out using an atomic force microscope located in the laboratory 135, Block C4. Figure 16 shows the instrument with sample under the cover and the screen showing the process of scanning.

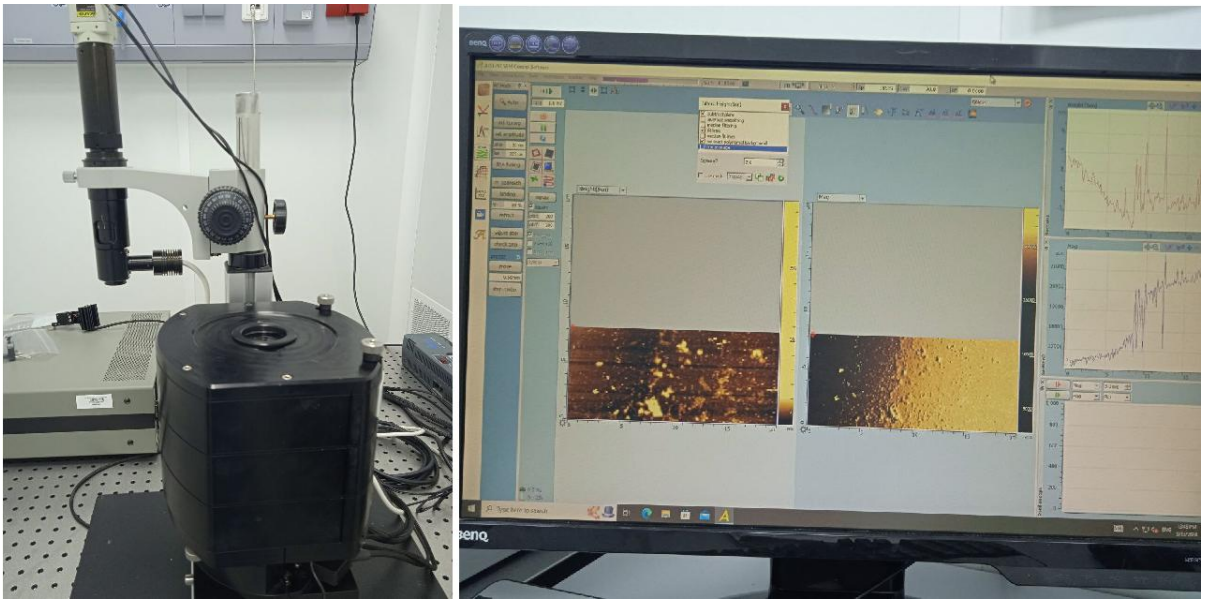

Figure 16: AFM imaging: setup and the screen.

Due to time constraints the AFM imaging was not conducted on the second stage of the experiment, different more available controls were used instead. It is feasible to conduct AFM when this work is continued because the protocol developed is novel and there are several parameters which can influence its performance, each of which can give different results and in order to find the best ones it would be necessary to perform the AFM too.

Chapter 3 – (RESULTS)

3.1 Detection of samples

As described in Chapter 2. Materials and methods there were fabricated constructive batches of sensors which later underwent functionalization procedure. After that the detection was carried out in respect to the three sample variants described above. Detection includes 20 minutes observation while saving data points each minute. Data points are the current RI reading of the sensor (each peak and valley) which depend on the binding of the target molecule to the sensor.

All in all, there are 7 detection steps each 20 minutes long: pure PBS, and 6 concentrations of the sample which are defined in each case separately (see above).

Three samples prepared under markedly different conditions as described in sections above underwent detection procedure using OFS functionalized with antibodies to amyloid beta or biotinylated and pegylated amyloid beta 42 peptide (custom made).

As the continuation and expansion of the original experiment two more detection steps were carried out starting from Detection 4, partially they were needed because of the poor quality of several previous runs but allowed also a possibility to expand the scope of the experiment. First, the sample preparation and detection were carried out as described recently, then the new step was added. The new step consisted in measurement of arbitrarily “unknown” concentrations: originally sample is prepared in serial dilution which each consecutive sample having concentration 10 times less than previous, 11 concentrations in total, but only 6 are used for detection (1, 3, 5, 7, 9, 11) with concentration 1 being the lowest. On this step instead of discarding unused concentrations we performed an additional round of detection which was conducted the following way:

- Probes were fabricated and functionalized according to the standard protocol;

- Two “unknown” concentrations were selected from the unused ones (stored in reference files);
- For each concentration there were assigned a functionalized sensor and a reference sensor (fabricated, calibrated, not functionalized)

During the second stage of the experiment, additional validation steps are undertaken as follows to ensure efficiency of the modified functionalization protocol. During the first functionalization using peptides as BREs, total amount of 12 fabricated and calibrated probes were used. Six (6) probes were selected for routine detection procedure, six remaining were divided into two groups: 3 probes functionalized with streptavidin and blocked with MPEG, without biotinylated peptides, and another 3 probes extracted from the functionalization procedure before grafting streptavidin. This was made to compare first readings of the probes and to see possible differences depending on the marked differences of the probes.

The raw data and code used to analyze it are uploaded to the google disc and can be found using the link to Google drive attached in Chapter 1.

Number	Date	Target	BRE	BRE conc.	Target	Notes
1	21.10.2024	Abeta 42 peptide (immediate use)	Antibody	4 ug/mL	ABeta42 (stock)	Standard serial solution
2	03.11.2024	Abeta 42 peptide (incubated overnight in PBS)	Antibody	4 ug/mL	ABeta42 (stock)	Standard serial solution
3	18.11.2024	Abeta 42 peptide (incubated overnight in PBS 2x diluted with DI water)	Antibody	4 ug/mL	ABeta42 (stock)	Standard serial solution
4.1	21.12.2024	Abeta 42 peptide (incubated overnight in PBS) Rerun	Antibody	4 ug/mL	ABeta42 (stock)	Standard serial solution
4.2	21.12.2024	Abeta 42 peptide (incubated overnight in PBS) Rerun	Antibody	4 ug/mL	ABeta42 (stock)	Uknown concentrations
5.1	23.12.2024	Abeta 42 peptide (immediate use) Rerun	Antibody	4 ug/mL	ABeta42 (stock)	Standard serial solution
5.2	23.12.2024	Abeta 42 peptide (immediate use) Rerun	Antibody	4 ug/mL	ABeta42 (stock)	Uknown concentrations
6.1	20.02.2025	Abeta 42 peptide (immediate use)	Biotinylated peptide	2 ug/mL	ABeta42 (stock)	Standard serial solution
6.2	20.02.2025	Abeta 42 peptide (immediate use)	Biotinylated peptide	2 ug/mL	ABeta42 (stock)	Uknown concentrations
7	21.02.2025	Abeta 42 peptide (immediate use)	Biotinylated peptide	Control (see details)	ABeta42 (stock)	Control
8.1	02.03.2025	Abeta 42 peptide (immediate use)	Biotinylated peptide	3 ug/mL	ABeta42 (stock)	Standard serial solution
8.2	02.03.2025	Abeta 42 peptide (immediate use)	Biotinylated peptide	3 ug/mL	ABeta42 (stock)	Uknown concentrations
9.1	03.03.2025	Abeta 42 peptide (immediate use)	Biotinylated peptide	4 ug/mL	ABeta42 (stock)	Standard serial solution
9.2	03.03.2025	Abeta 42 peptide (immediate use)	Biotinylated peptide	4 ug/mL	ABeta42 (stock)	Uknown concentrations
10.1		Abeta 42 peptide (immediate use)	Biotinylated peptide (without biotin blockage for control)	3 ug/mL	ABeta42 (stock)	Standard serial solution

10.2	Abeta 42 peptide (immediate use)	Biotinylated peptide (without biotin blockage for control)	3 ug/mL	ABeta42 (stock)	Uknown concentrations
11.1	Abeta 42 peptide (incubated overnight in PBS)	Biotinylated peptide	4 ug/mL	ABeta42 (stock)	Standard serial solution
11.2	Abeta 42 peptide (incubated overnight in PBS)	Biotinylated peptide	4 ug/mL	ABeta42 (stock)	Uknown concentrations
12.1	Abeta 42 peptide (incubated overnight in PBS 2x diluted with DI water)	Biotinylated peptide	4 ug/mL	ABeta42 (stock)	Standard serial solution
12.2	Abeta 42 peptide (incubated overnight in PBS 2x diluted with DI water)	Biotinylated peptide	4 ug/mL	ABeta42 (stock)	Uknown concentrations

Table 4: Measurements in chronological order

3.1.1 Serial solution detection results

The data acquired in this step is stored on the Google disc (https://drive.google.com/drive/folders/1vN-0xt0lchyjZg-MMz8VnLIn_wUqr_Rx?usp=sharing), as well as software used for initial analysis to ensure that BRE fulfils the goal of the target detection. All the consequent steps of Data analysis are described in Section 3.2.

Here are some representative examples of data collected to show how it looks like on the initial stage.

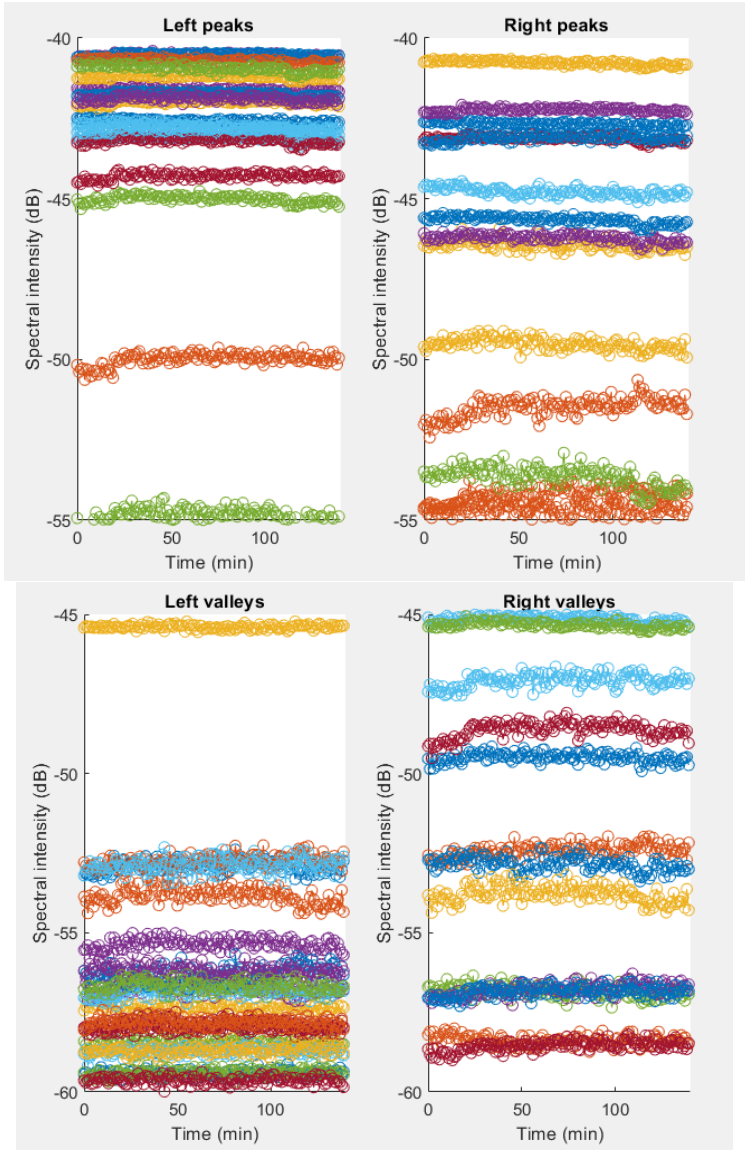

Antibodies

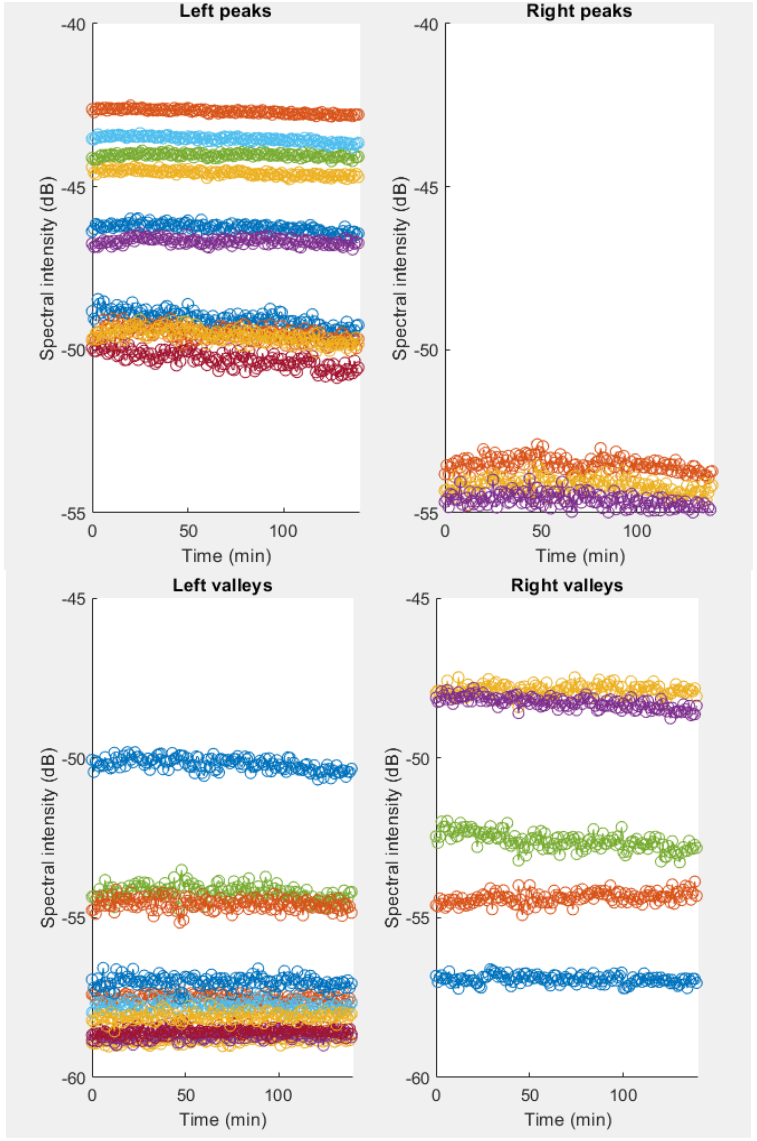

Peptides

Figure 17: Detection graphic results Left and right peaks and valleys (raw) ABs Det 5.1 (a), Peptides Det 9.1 (b)

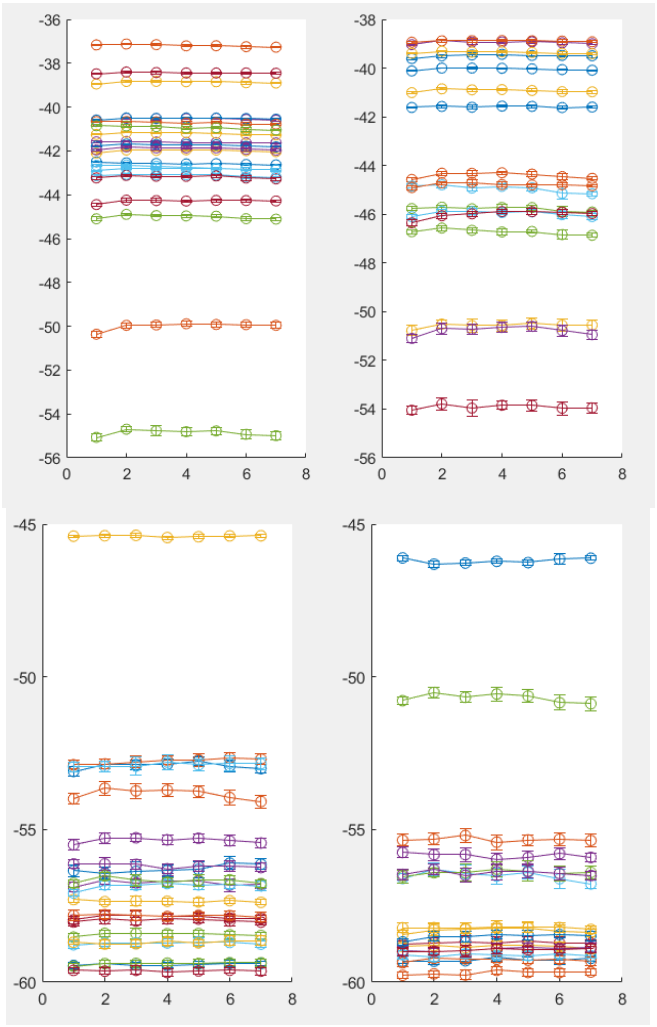

Antibodies

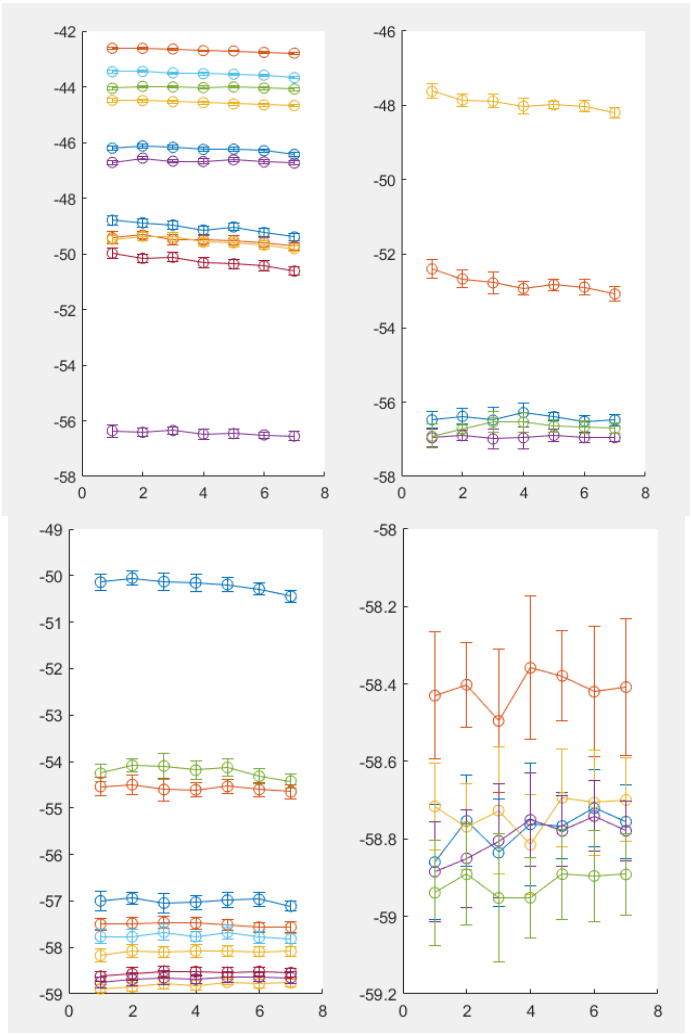

Peptides

Figure 18: Detection graphic results Left and right peaks and valleys (averages) ABs Det 5.1 (a), Peptides Det 9.1 (b)

3.1.2 Additional detection step results

On this step 1-2 unknown concentrations left after the routine detection were analyzed, below is the graphic representation of the result produced using the fist stage analysis. The better picture is expected upon application of the second stage analysis.

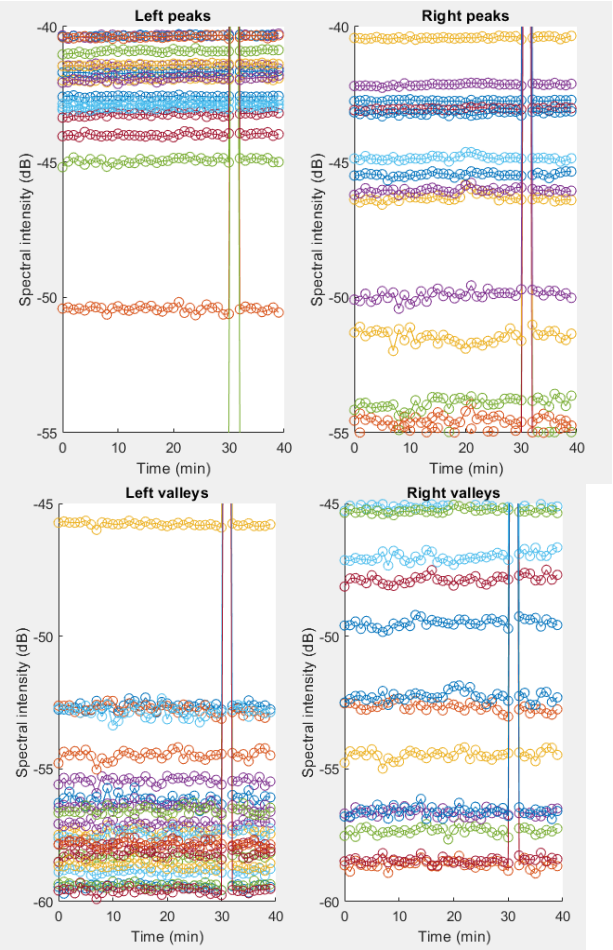

Antibodies

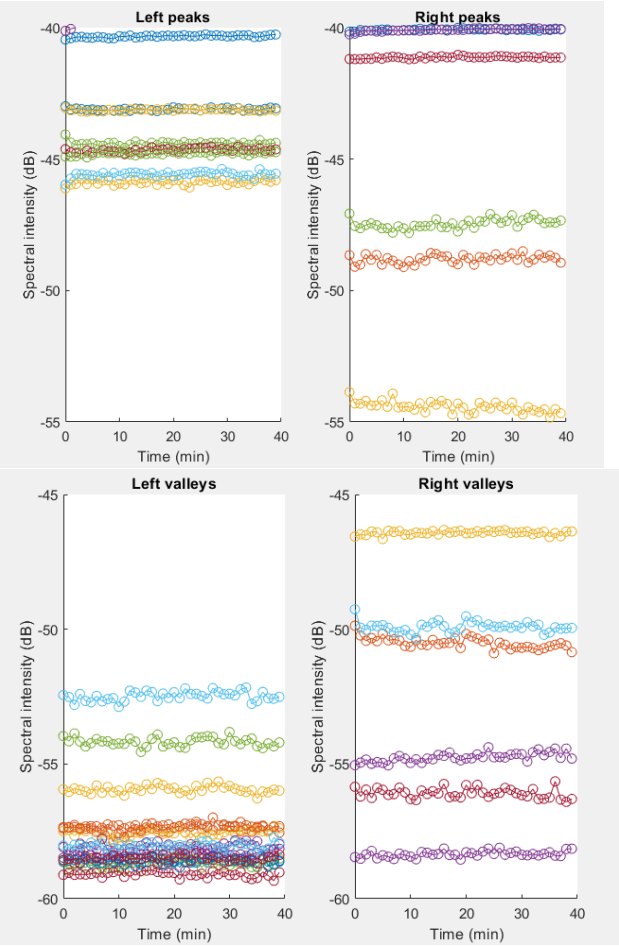

Peptides

Figure 19: Unknown concentrations (raw) Detection graphic results Left and right peaks and valleys (raw) ABs Det 5.2 (a), Peptides Det 9.2 (b)

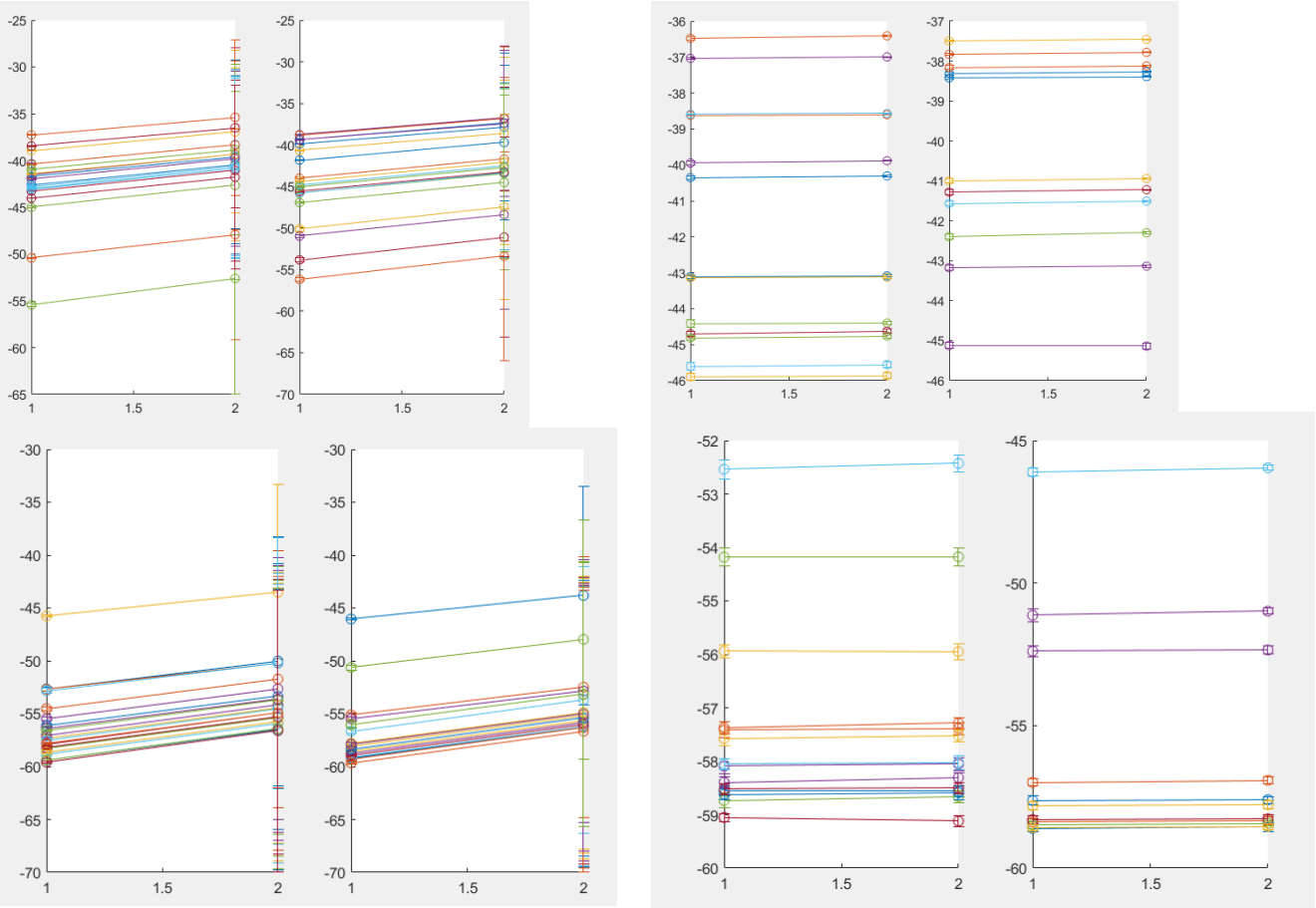

Antibodies **Peptides**

Figure 20: Unknown concentrations (averaged) Detection graphic results Left and right peaks and valleys (average) ABs Det 5.2 (a), Peptides Det 9.2 (b)

3.2 Data analysis

The task of the analysis is primarily to prove the sensitivity of peptides in RI sensing as well as to find a difference in characteristics of the RI changes in respect to the different nature of the sample used in each case, as well as characteristic differences between antibodies and peptides as BREs. There is a plan to check two possibilities:

- Define the kinetics of binding through several concentrations to see if there is a noticeable and reproducible change in it depending on the nature of the sample.
- Define whether it is possible to find a correlation between the RI change pattern of different peaks/valleys and the nature of the target.

So far there is only the usual pipeline available showing the change in RI upon binding of the target, the new pipeline is under development. As the new detection protocol was introduced the code in Python will be modified accordingly.

The results of data analysis are presented in the form of the most important graphs; raw data and scripts are readily available at the link given above.

3.2.1 Calibration data analysis

The general procedure of data analysis is as follows: first calibration data are analyzed, and the most sensitive probes are chosen for further functionalization.

The OFS used in this work has a unique characteristic of several spectral features serving as a combined array of probes.

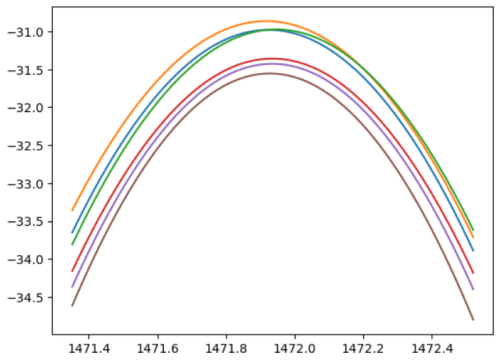

Figure 21: Example of a separate peak

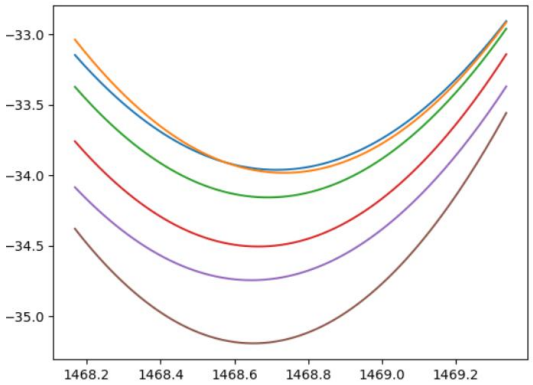

Figure 22: Example of a valley

Therefore, there is a possibility to explore different ways to interpret such data. As we can see a separate peak of value looks like a read out of a single sensor, for example in case of an electrochemical one we would have a single line differing depending on analyte concentrations, like in the Figure below

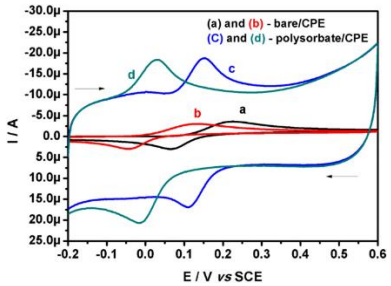

Figure 23: Electrochemical sensor results, graphical form. Adapted from [36]

To extract the probe signature mentioned above we applied data analysis script to the calibration data.

3.2.2 Probe signature

To obtain probe signatures we analyzed two instances of calibration and detection.

We chose to use data from Detection 9.1 and following probes:

- LV37 (Calibration 3 - Channel 1/Detection 9.1 – Channel 1)
- LV35 (Calibration 3 – Channel 3/Detection 9.1 – Channel 6)

For the initial step we chose to use peaks on the left from FBG spectrum. During calibration MATLAB function findpeaks outputs locations of detected peaks and stores them in variable called pre_peak_locs, which contains all peaks before the most sensitive ones are chosen. We used this variable as opposed to good_peak_locs since during detection all peaks are registered.

In the case of probe LV 35 we found the following correspondence to LocPeakLeft from the Detection procedure:

	Peak location						
LocPeakLeft	81	652	1008	1437	1715	1952	2332
pre_peak_locs	102	659	1011	1453	1720	1962	2347
Deviation	21	7	3	16	5	10	15

Table 5: Correspondence of peaks, LV35, Detection 9.1

In the case of LV37 correspondence was observable but variation was wider

	Peak location						
LocPeakLeft	--	--	384	1121	1884	3287	3988
pre_peak_locs	31	54	439	1194	1945	3337	4000
Deviation	--	--	55	73	61	50	12

Table 6. Correspondence of peaks, LV37, Detection 9.1

As we can see existing correspondence allows us to draw a parallel and create a probe signature which consequently can be used for data analysis.

The procedure described below is simple and is supposed to serve as a basis for further development which can naturally include machine learning approaches, one of which is discussed

later.

The MATLAB script was modified to save necessary data in a .csv file labeled with code name of the probe to ensure ease of management further and traceability. Added lines:

- In beginning, for input of the probe code and other necessary information:

```
% Modification for probe signature creation

code_name = "LV37";
set = 3;
probe_name = strcat(code_name, '_Set', num2str(set), '_Chan', num2str(sensor_trace));
```

- Saving data:

```
% Modifications for probe signature creation

writematrix(pre_peak_locs, strcat(probe_name, '_pre_peak_locs', '.csv'))
writematrix(pre_valley_locs, strcat(probe_name, '_pre_valley_locs', '.csv'))
writematrix(sens_peaks, strcat(probe_name, '_sens_peaks', '.csv'))
writematrix(sens_valleys, strcat(probe_name, '_sens_valleys', '.csv'))
```

These steps make it easy to retrieve necessary information upon request without the need to run calibration script again. This is implemented in MATLAB but can also be done using Python script developed by a fellow researcher recently (can also be found on Google disc), we chose MATLAB because it is faster to run these two first steps. The saved data then can be easily retrieved in the Python script.

For our further analysis we saved the following data:

From the calibration script, we saved the following tables:

- pre_peak_locs – indices of peaks detected
- pre_valley_locs – indices of valleys detected
- sens_peaks – sensitivities of peaks before differentiating
- sens_valleys – sensitivities of peaks before differentiating

We also introduced several modifications in the MATLAB data analysis script:

Creating unique code name:

```
% Modification for probe signature application later
detection = "9.1";
code_name = "LV35";
chan = strcat(ChannelData);
probe_name = strcat('Detection_', detection, '_', code_name, '_', chan);
```

Saving data:

```
% Locs
writematrix(LocPeakLeft, strcat(probe_name(1,:), '_LocPeakLeft', '.csv'))
writematrix(LocPeakRight, strcat(probe_name(1,:), '_LocPeakRight', '.csv'))
writematrix(LocValleyLeft, strcat(probe_name(1,:), '_LocValleyLeft', '.csv'))
writematrix(LocValleyRight, strcat(probe_name(1,:), '_LocValleyRight', '.csv'))
% Responses
writematrix(ResponsePeakLeft, strcat(probe_name(1,:), '_ResponsePeakLeft', '.csv'))
writematrix(ResponsePeakRight, strcat(probe_name(1,:), '_ResponsePeakRight', '.csv'))
writematrix(ResponseValleyLeft, strcat(probe_name(1,:), '_ResponseValleyLeft', '.csv'))
writematrix(ResponseValleyRight, strcat(probe_name(1,:), '_ResponseValleyRight', '.csv'))
```

From the data analysis script, we save following tables:

- LocPeakLeft
- LocPeakRight
- LocValleyLeft
- LocValleyRight
- ResponsePeakLeft
- ResponsePeakRight

- ResponseValleyLeft
- ResponseValleyRight

These tables are saved as .csv files with indication of probe code name and set (if available) to ensure traceability. These files are uploaded to the Google drive and can be used on the next data analysis step in Python scripts which are also available.

3.2.3 Statistical significance in detection

In order to prove the proper functioning of our probes we performed a series of comparisons with controls. Full data is available at Google drive (link given above, folder “Statistical comparison between controls and probes”).

At this stage of the experiment this control procedure was deemed the best choice based on estimation of available time and resources, other possible procedures to further validate performance are planned for the future steps beyond the current thesis. Here we give graphic representation of the performed comparisons as well as p-value and T-statistics for several pairs of probes undergoing different procedures. As was mentioned in the “Calibration data analysis”, the unique feature of the used probes is that they each cab be treated as an array of probes with different sensitivities (which we now can define due to the probe signature).

First, I performed analysis of data before application of probe signature approach described above and after that to highlight the significant difference, the data is presented in the following subsections.

3.2.3.1 Evaluation of variability between the probes

The semi distributed interferometric sensors used have inherent stochasticity and to define what threshold to consider significant we first have to see the intra-batch variability; this is connected to the fact that each probe can be treated as an array of very closely spaced sensors with different sensitivities.

Comparison between the bare probes from the same batch

Comparison between the probes functionalized with antibodies from the same detection run

1. The variability between the bare probes (LV29REF and LV25REF)

Peaks and valleys of bare probes before application of probe signature

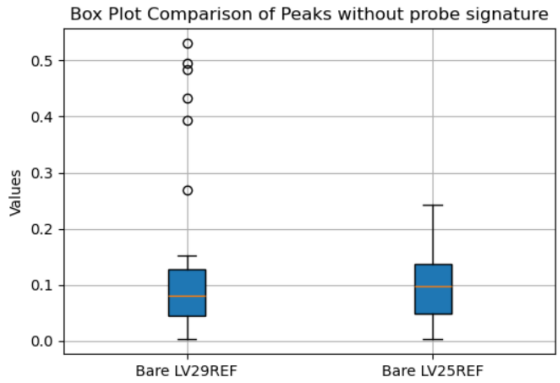

T-statistic: 1.1504986651650875
P-value: 0.2529201868798299

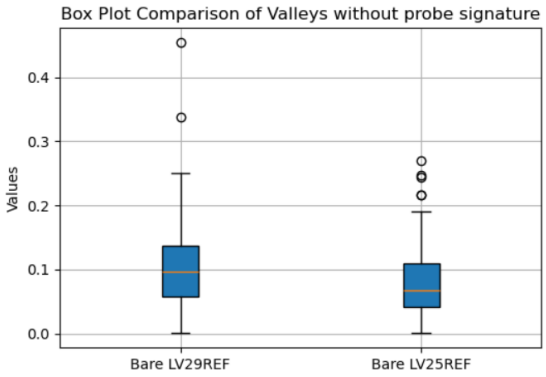

T-statistic: 1.9600704182693514
P-value: 0.053013474379915805

Figure 24: Comparison of the bare probes in detection without probe signature (probes LV29REF and LV25REF)

Peaks and valleys of the same bare probes after application of probe signature. Here the lower limit for sensitivity was 15 (absolute value), it can be increased or decreased according to the need. How it affects the analysis we will describe later.

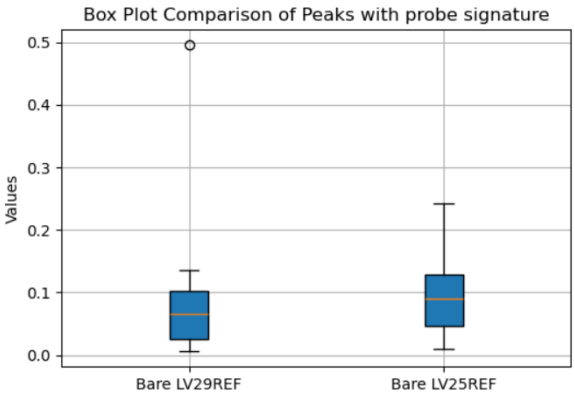

T-statistic: -0.8242072599324253
P-value: 0.4126618319995141

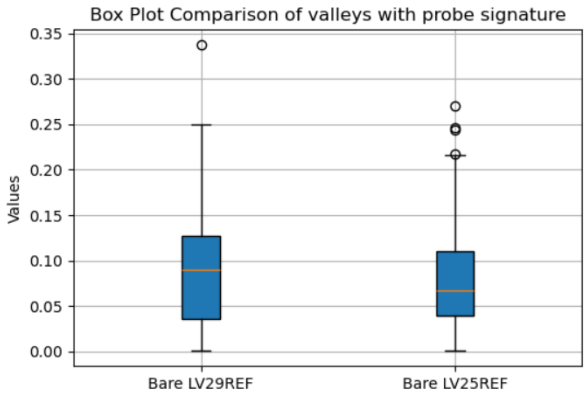

T-statistic: 0.63856136217492
P-value: 0.5254986598056648

Figure 25: Comparison of the bare probes in detection with probe signature, threshold = 15 (probes LV29REF and LV25REF)

Sensitivity threshold: 30, same probes

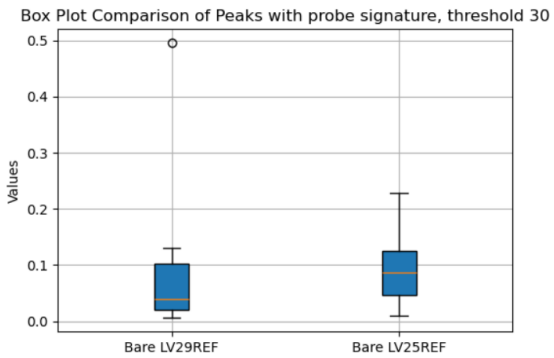

T-statistic: -0.45330220860647275
P-value: 0.6520521526876901

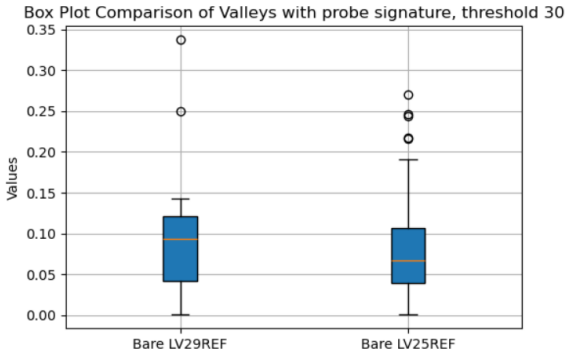

T-statistic: 0.7750969946117854
P-value: 0.4415430903382713

Figure 26: Comparison of the bare probes in detection with probe signature, threshold = 30 (probes LV29REF and LV25REF)

It is obvious that probe signature implementation increased the reliability of the data, affecting both T-statistics and p-value. This is because before probe signature application all responses are considered, probe signature in its turn is used in a specifically designed function to leave only peaks with known and good sensitivity (can be adjusted by demand), thus significantly reducing noise level and increasing signal to noise ratio, which is extremely important for such probes. After implementation of probe signature, we see that bare probes have insignificant differences (p-value 0.41 and 0.53), on the other hand before probe signature is implemented the noisy data gave smaller p-values (P-value: 0.26 and 0.053).

There is another set of controls in addition to the bare probes: probes functionalized only with streptavidin and undergone the same detection procedure. Their results are the following:

1. Peaks and valleys before application of the probe signature. Probes LV21 and LV 26.

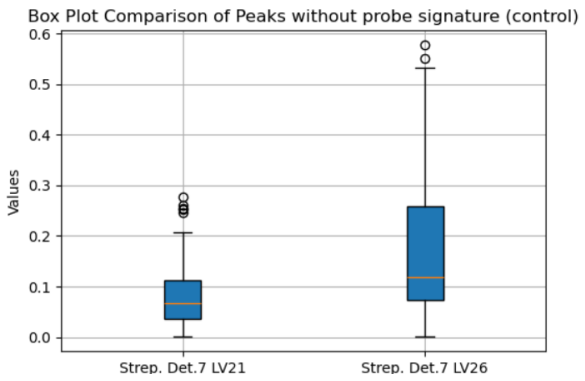

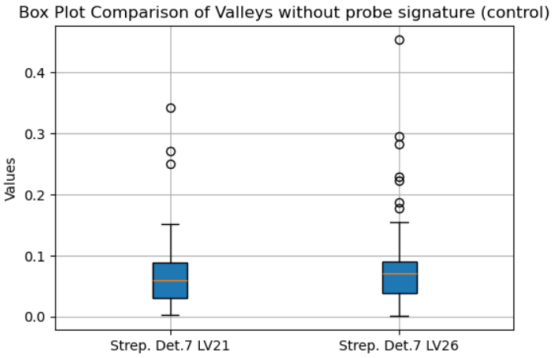

T-statistic: -4.162824743139172
P-value: 5.730935022085494e-05

T-statistic: -0.7693366924432415
P-value: 0.44309984055297025

Figure 27: Comparison of the streptavidin probes in detection without probe signature (Probes LV21 and LV 26)

2. Peaks and valleys after application of the probe signature. Probes LV21 and LV 26. Threshold 15

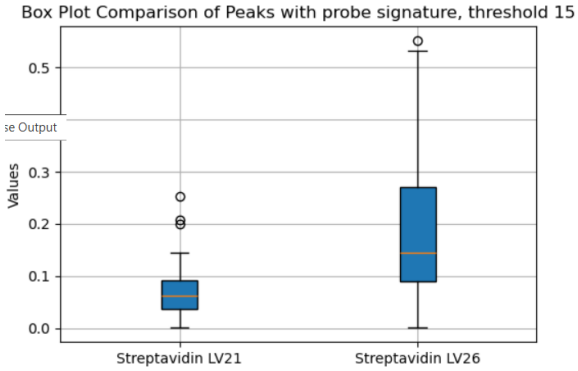

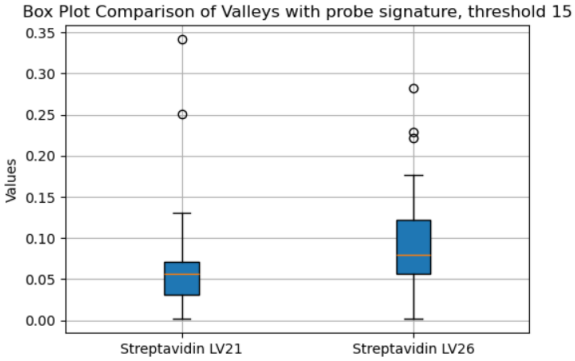

T-statistic: -4.80330602148803
P-value: 6.542629815105271e-06

T-statistic: -1.5687690384173327
P-value: 0.12233553576714572

Figure 28: Comparison of the streptavidin probes in detection with probe signature, threshold = 15 (Probes LV21 and LV 26)

3. Peaks and valleys after application of the probe signature. Probes LV21 and LV 26. Threshold 30

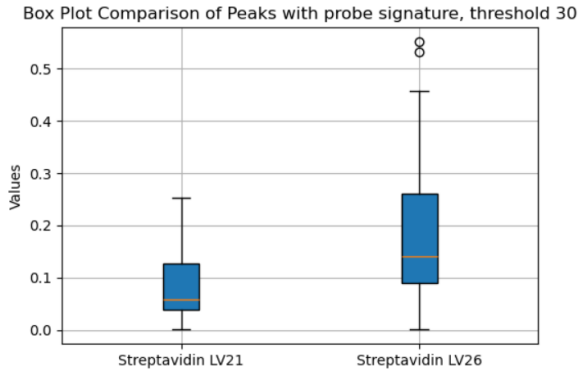

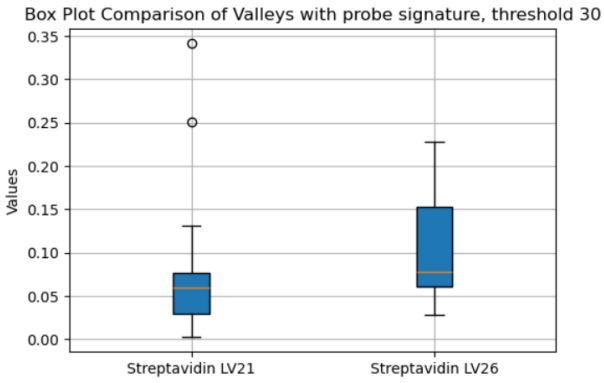

T-statistic: -3.4970552195639364

T-statistic: -1.431529592137511

P-value: 0.0008100487999987392 P-value: 0.16004613141593035

Figure 29: Comparison of the streptavidin probes in detection with probe signature, threshold = 30 (Probes LV21 and LV 26)

The same procedure was applied to functionalized probes to make sure correspondence remains valid for them too:

Peaks and valleys of probes functionalized with antibodies (Detection 5) before application of probe signature

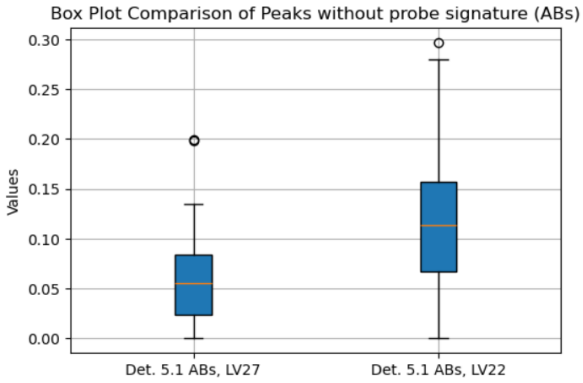

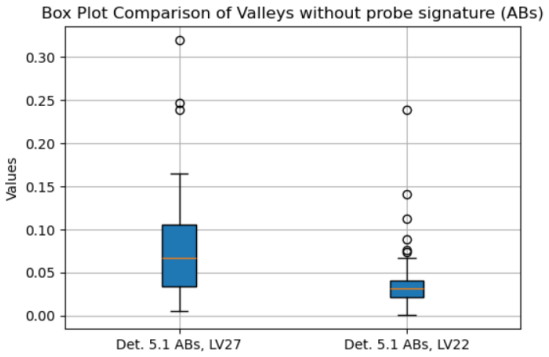

T-statistic: -5.031429820749929
P-value: 1.953692474628059e-06

T-statistic: 4.388174777123126
P-value: 2.6339086237766453e-05

Figure 30: Comparison of the streptavidin probes in detection without probe signature (Probes LV27 and LV 22)

Peaks and valleys of probes functionalized with antibodies (Detection 5) after application of probe signature, threshold 15.

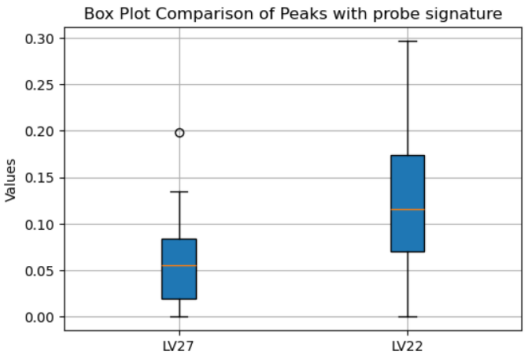

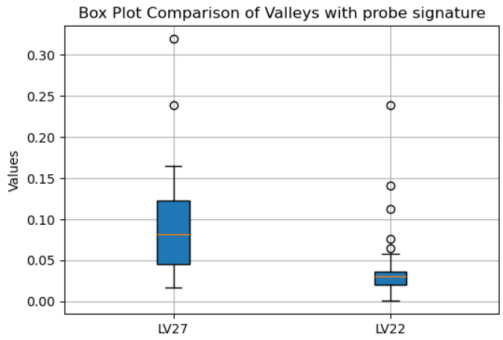

T-statistic: -4.8115808383707295
P-value: 7.701473964167582e-06

T-statistic: 3.7699138507042425
P-value: 0.0003898500742735120 5

Figure 31: Comparison of the streptavidin probes in detection with probe signature, threshold

= 15 (Probes LV27 and LV 22)

Peaks and valleys of probes functionalized with antibodies (Detection 5) after application of probe signature, threshold 30

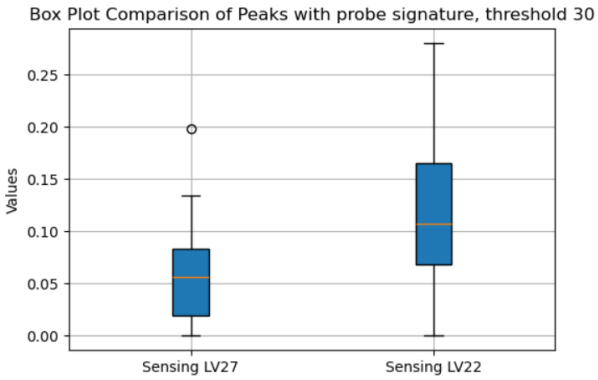

T-statistic: -4.152133188932583
P-value: 9.651673753681542e-05

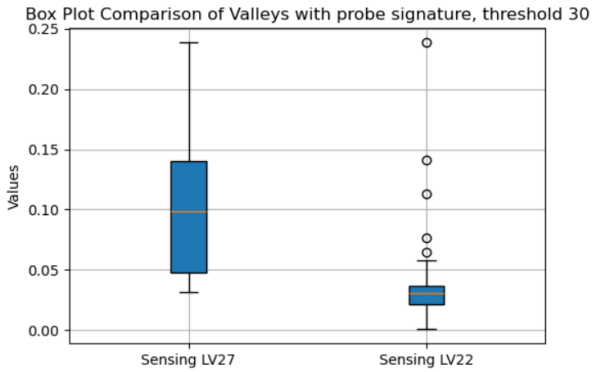

T-statistic: 4.098785635175646
P-value: 0.00016303088392517732

Figure 32: Comparison of the streptavidin probes in detection with probe signature, threshold = 30 (Probes LV27 and LV 22)

As we can see the greater threshold can lead to more variability between the probes from the same detection run and less variability between the control probes, this contrasting behavior further underscores their differences and ampleness of data which can be extracted from the probes functionalized with BRE, as well as justifies use of peaks and valleys in one sensor as an array of sensors because simple averaging is not feasible in these settings.

Possible reasons for such heterogeneity can be found in the nature of antibody and the way it binds to our sensor.

The same set of comparisons for probes functionalized with peptides (from Detection 9.1, probes LV37 and LV35).

Peaks and valleys of probes functionalized with biotinylated peptides (Detection 9.1) before application of probe signature

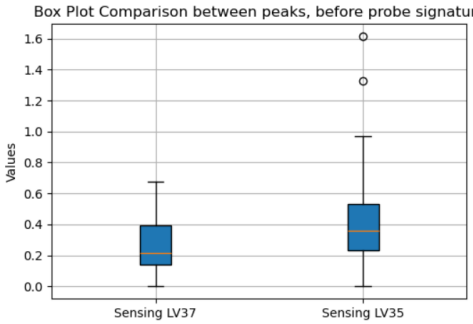

T-statistic: -1.6554798339866295
P-value: 0.10362815051273207

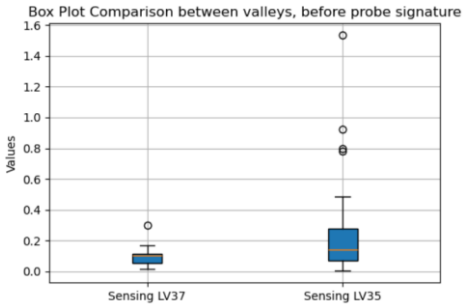

T-statistic: -1.9018266958518273
P-value: 0.06263504724271658

Figure 33: Comparison of the sensing probes with peptides as BRE in detection without probe signature (probes LV37 and LV35)

Peaks and valleys of probes functionalized with biotinylated peptides (Detection 9.1) after application of probe signature, threshold 15.

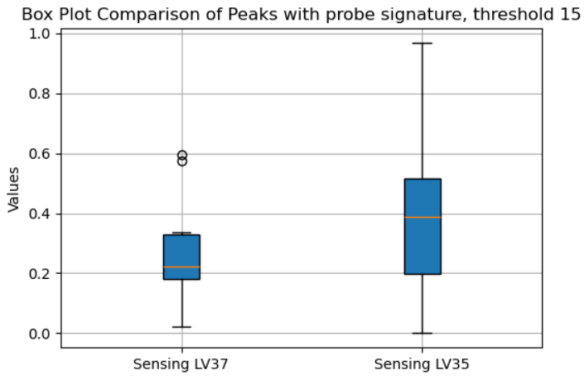

T-statistic: -1.357580641194584
P-value: 0.18304647576585642

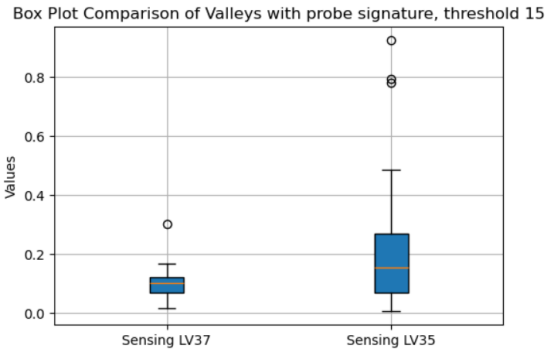

T-statistic: -1.6645614136544291
P-value: 0.10327167089357131

Figure 34: Comparison of the sensing probes with peptides as BRE in detection with probe signature, threshold = 15 (probes LV37 and LV35)

Peaks and valleys of probes functionalized with biotinylated peptides (Detection 9.1) after application of probe signature, threshold 30.

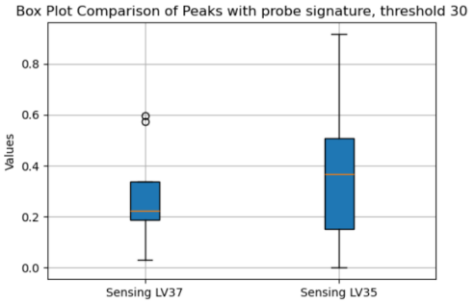

T-statistic: -0.6319849546406963
P-value: 0.5331340586183779

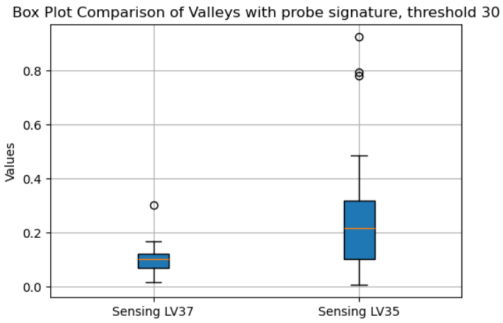

T-statistic: -2.0464495744690008
P-value: 0.04786650682861279

Figure 35: Comparison of the sensing probes with peptides as BRE in detection with probe signature, threshold = 30 (probes LV37 and LV35)

It is remarkable that in case of probes functionalized with peptides instead of antibodies the intra-run inter-probe variability is mostly statistically insignificant despite the different thresholds. This suggests presence of fundamental difference between the antibodies and peptides as BRE which deserves further investigation.

3.2.3.2 Bare probe vs antibodies

Here the two probes were compared: bare probe and probe functionalized with antibodies against amyloid beta 42. From now on we use data only after application of probe signature.

The probes were used for a standard detection procedure described above. The bare probe was used right after fabrication without any modification which in addition to serving as control for the functionalized probe also served as a control of the medium refractive index, to guarantee that functionalized probe does not show changes in the general RI, not based on the target binding. For this I saved response data from the script ScriptDataAmalysis.m. There are seven concentrations used, responses are averages over 20 minutes of observation, to ensure that bare and functionalized probes show different responses, we subtracted the value for the 1st concentration (pure PBS) from the value for the 7th (the highest), then absolute value was taken for further analysis. The hypothesis is that if functionalized probe is functional there should be a statistically significant difference

between the two (as was mentioned above the difference between reference probes was proven to be not statistically significant). We randomly chose the probes on the previous step and will use this data in the following, nevertheless the scripts and raw data are readily available, so it is possible to run any additional comparison on demand.

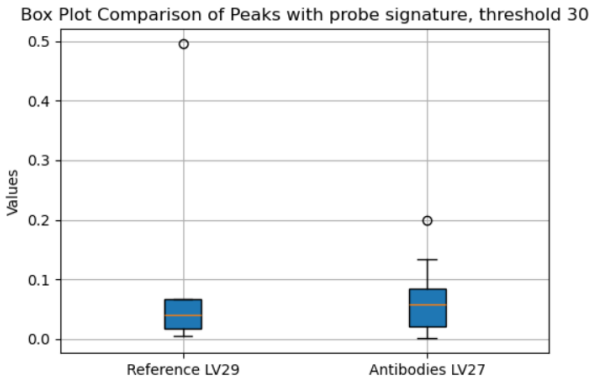

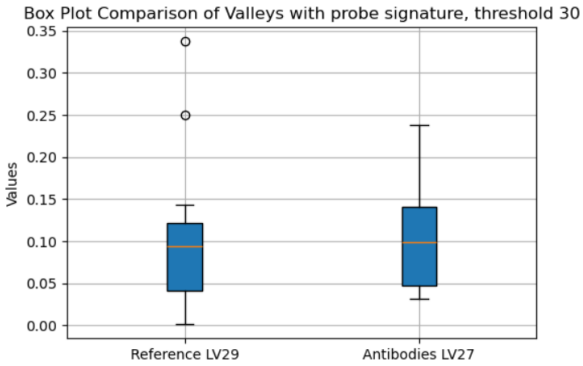

T-statistic: 1.0882110571362529
P-value: 0.2818255563908

T-statistic: -0.058434690029160775
P-value: 0.9538327254508593

Figure 36: Comparison of bare vs antibodies, with probe signature, threshold = 30 (probes LV29REF and LV27)

Results depicted graphically in Figure 36 show that surprisingly there was no significant difference between the bare probe and probe functionalized with antibodies. Possible explanations are the defect during functionalization or too stochastic binding of antibodies.

3.2.3.3 Bare probe vs peptide

Bare probe vs peptide, 4 ug/ml (Sensing probe: Detection 9.1, LV35 (Ch6), Reference probe: Detection 6.1, REFLV29 (Ch1), without functionalization)

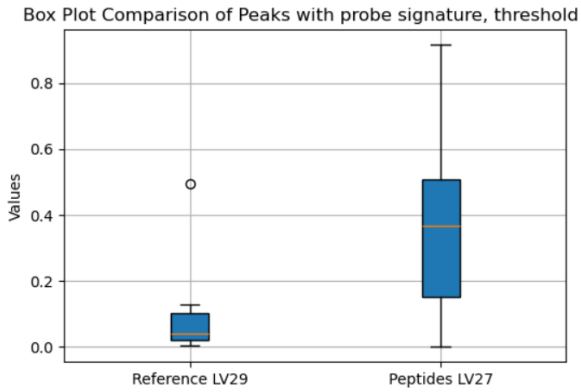

T-statistic: -3.5806623175237235
P-value: 0.0012323502591819258

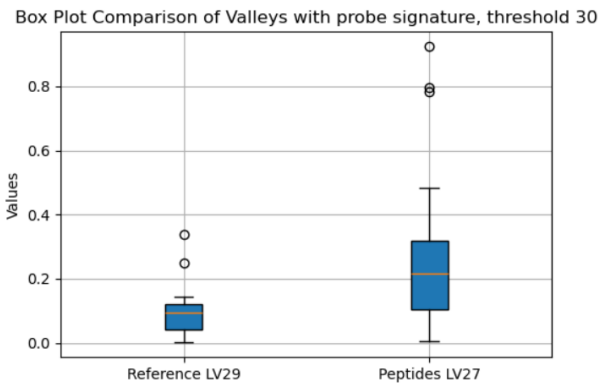

T-statistic: -2.575846872194381
P-value: 0.013608073419107143

Figure 37: Comparison of bare vs peptides, with probe signature, threshold = 30 (probes LV29REF and LV35)

Results depicted in Figure 37 show statistically significant differences between the bare probe and the probe functionalized with biotinylated peptides. This is in the stark contrast with the antibodies shown in the previous section further underlining feasibility to use peptides as BREs.

3.2.4 Further data analysis using probe signature to differentiate between "strains"

The next step is to use probe signatures for further data analysis trying to differentiate between the amyloid "strains". As mentioned, we used three variants of samples with varying incubation conditions to make sure aggregates formed with high probability have differences.

For data analysis we will use the first two concentrations (pure PBS without target, and the smallest concentration of the target, e.i. last in serial dilution). This is made to eliminate possible confounding effects, however small they may be, which can arise due to stepwise target binding on the latter steps which potentially can influence the overall picture.

In the data analysis MATLAB script, we made modifications to save responses only for the first two concentrations and only for detected peaks and valleys. Further this information can be seamlessly

incorporated into the approach described above in regards to probe signature assignment.

For further analysis we used randomly chosen probes from Detection 9.1 (peptides, stock, immediate use), Detection 10.1 (peptides, stock, overnight incubation in PBS), and Detection 11.1 (peptides, stock, overnight incubation in PBS 2X diluted in DI water). For convenience from now on we will call sample 1 (from stock) – Strain 1, sample incubated overnight in PBS – Strain 2, sample incubated overnight in diluted PBS 2X in DI water – Strain 3. To further decrease possible variability we compare only probes connected to Channel 1 across all runs.

For this section we modified original function in Python which now allows to analyze every spectral feature response separately. For this we get the final table of sensitivities and responses for the three probes analyzed in the following. Manually (can be automated later) we chose one feature with similar sensitivity in each case. Namely:

- LV35 we chose peak 5 with sensitivity -127.124;
- LV42 we chose peak 21 with sensitivity -121.853;
- LV49 we chose peak 33 with sensitivity -122.662

In case of valleys:

- LV35 we chose valley 3 with sensitivity 84.804
- LV42 we chose valley 0 with sensitivity -82.046
- LV49 we chose valley 7 with sensitivity -83.379

3.2.4.1 Comparison between Detection 9.1 (strain 1) and Detection 11.1 (strain 2)

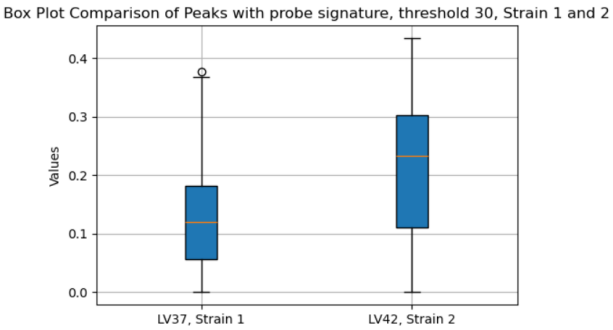

T-statistic: 5.094066204342764
P-value: 2.3791419794696723e-06

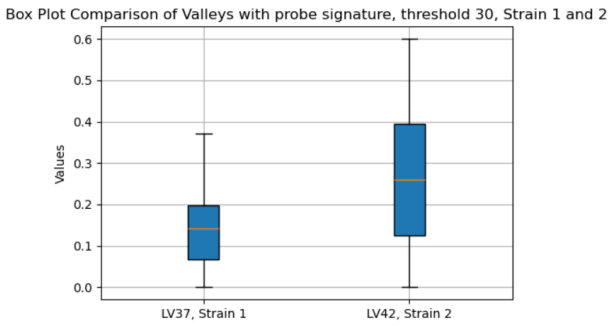

T-statistic: 6.671829590957109
P-value: 3.2948603411044716e-09

Figure 38: Comparison of Strain 1 vs Strain 2, with probe signature, threshold = 30 (probes LV37 (D9.1) and LV42 (D11.1))

Results show statistically significant differences between different strains in the case of features with comparable sensitivity warranting further investigation.

3.2.4.2 Comparison between Detection 9.1 (Strain 1) and Detection 12.1 (Strain 3)

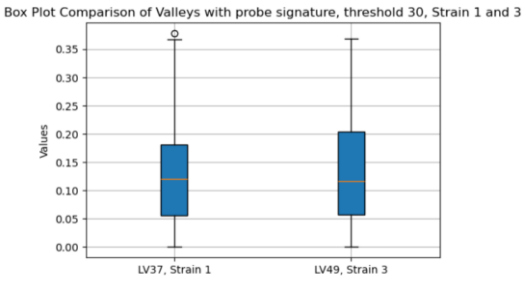

T-statistic: 1.3726104588863604
P-value: 0.17380741450233517

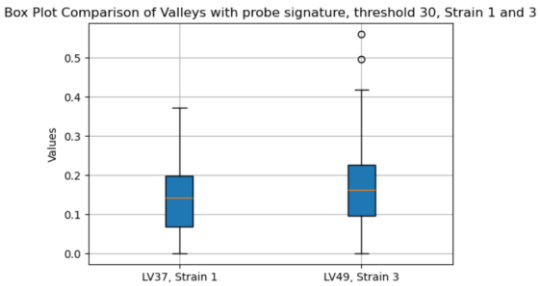

T-statistic: 8.712712304562151
P-value: 3.896750477273029e-13

Figure 39: Comparison of Strain 1 vs Strain 3, with probe signature, threshold = 30 (probes LV37 (D9.1) and LV49 (D12.1))

Results surprisingly show insignificant differences in case of the peak and very significant differences in case of the valley, such artefacts are expectable within the framework of the inherent stochasticity of the sensors used. Nevertheless, this effect can be reduced by adjusting and taking into account multiple features, which can be done in the continuation of this work.

3.2.4.3 Comparison between Detection 11.1 (Strain 2) and Detection 12.1 (Strain 3)

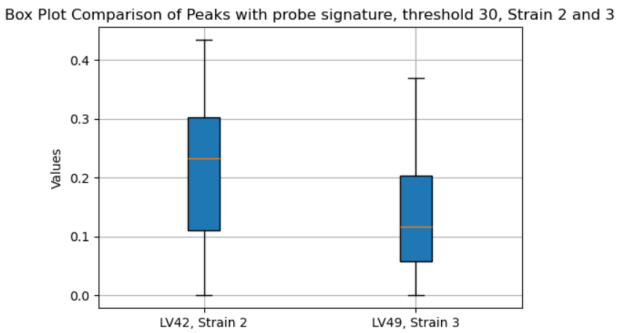

T-statistic: -3.7086537019110817
P-value: 0.0003883082088240463

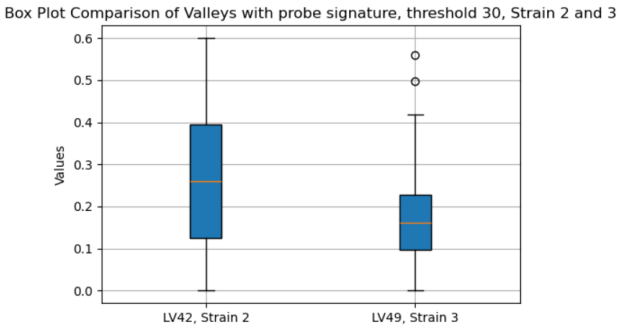

T-statistic: -0.3987750918256392
P-value: 0.6911485409888531

Figure 40: Comparison of Strain 2 vs Strain 3, with probe signature, threshold = 30 (probes LV42 (D11.1) and LV49 (D12.1))

Results show that the peaks show statistical differences, but valleys do not. This was to be expected since the very beginning of the experiment valleys appeared to be less reliable.

3.2.5 Machine learning applications – defining "unknown" concentrations

Based on the data received using probe signature we created a preliminary ML model. For the initial step we used the most accessible ML library in Python, sklearn. The input was the table generated using files for sensitivity and responses

3.2.5.1 Machine learning models

```python
import pandas as pd
from sklearn.model_selection import train_test_split
from sklearn.linear_model import LinearRegression

# Example dataset (assuming one sensor per sensitivity)
data = {
    'Concentration': [0, 0.000000000001, 0.000000001, 0.00000001, 0.000001, 0.0001, 0.01],  # Input variable
    'Sensor_Response': LV35_peaks[0][3:],  # Target variable
    'Sensitivity': LV35_peaks[0][1] * 5  # Fixed sensitivity for this sensor
}

df = pd.DataFrame(data)

# Define features and target
X = df[['Concentration', 'Sensitivity']]  # Features: Concentration & Sensitivity
y = df['Sensor_Response']  # Target: Sensor response

# Split data
X_train, X_test, y_train, y_test = train_test_split(X, y, test_size=0.2, random_state=42)

# Train model
model = LinearRegression()
model.fit(X_train, y_train)

# Make predictions
y_pred = model.predict(X_test)

print(f"Predicted responses: {y_pred}")
```

```
Predicted responses: [-55.2336251 -55.2336251]
```

Figure 41: Example of ML code using sklearn

The current preliminary model shows unsatisfactory results with the following parameters:

- Mean Absolute Error: 2.7641631755685387
- Root Mean Squared Error: 3.455777048985985

The scatter plot between the predicted and actual responses is presented in Figure 42.

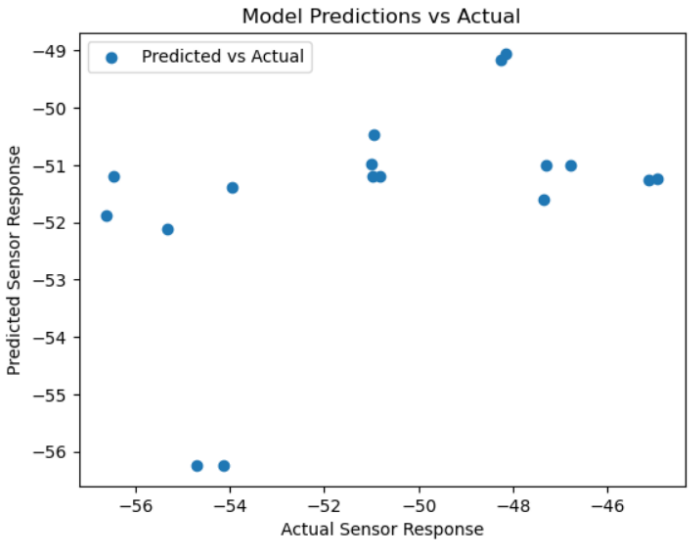

Figure 42: Model predictions vs actual responses

It is obvious that simple linear models are not well suited to this task, therefore we suggest using more sophisticated ML models for the future research in this direction. As was mentioned, the training of the model can be best accomplished using calibration data but for this now we lack some crucial data points as well as established correspondence between calibration solution RI change and concentrations of the analyte.

CHAPTER 4 - (DISCUSSION)

The curret work was comprised of two stages with the first traditional stage serving as a basis and reference for the second one which was more novel.

During the first stage several detections were conducted using validated functionalization and detection protocol. Data was collected and analyzed also using validated software instruments. At this stage the procedure was established, which consequently served as a basis for expansion for the second stage.

This thesis had one general hypothesis and goal and several smaller ones which contribute to the whole, these goals are once again listed below and discussed one by one:

4.1 Peptides as BRE

In the current work we validated use of biotinylated peptides instead of antibodies for detection of amyloid-beta peptide in the case refractive index semi distributed fiber optic biosensors as opposed to electrochemical and SPR biosensors which also use peptides. The results unequivocally prove that peptides also show sensitivity in the way antibodies do, although there is still further work needed in order to find the optimal concentration of BRE, modifications to the functionalization protocol can also be considered on the next step.

The sensors used in our lab already have the advantage of being economical and easy in fabrication, use of peptides will allow us to make them even more economical. For example, 100 uL of antibody against amyloid-beta costed 438 570 tenge, at the same time 10 mg (that is, much greater volume) of custom synthesized peptides biotinylated and with PEG-linker costed 334 374. Moreover, as peptides are short, they can be stored for longer time. The main concern with the current peptides is that they tend to aggregate but there is a procedure which can reverse the process and yield disaggregated

peptides ready for further use.

Further tentative advantage of the current work is the aligned distribution of BRE on the sensor surface. Creating an aligned as opposed to stochastic distribution of BRE on the surface of the sensor (as opposed to the most sensors mentioned in literature review as well as those used in our laboratory) can have certain advantages which are subject to further investigation.

4.2 Probe signature

Another achieved milestone of the current work was utilizing unique features of semi distributed optical biosensor to explore probability of novel data analysis ways. Using data generated on the steps of routine calibration and data analysis pipelines we created a probe signature approach which gives further flexibility to the data analysis allowing us to use only spectral features with certain sensitivity or set a sensitivity threshold. The advantages of this approach were demonstrated in the text of this work.

As a further development we envision use of probe signature in combination with more extensive calibration to better assess binding of the target to the probe. We propose to use ML to study the peaks and valley sensitivity on the stage of calibration, when RI changes uniformly, then find correspondence between the concentrations of analyte and calibration solution RI. Based on the differences between the predicted and observed responses we can hypothesize the tentative distribution of the bound target on the probe further enriching possibilities of data analysis.

4.3 Different strains

One of the goals was investigating possibility to differentiate between slightly different samples, “strains” of amyloid beta 42 (this is unique to diseases associated with aggregation since aggregates can have very different structures if aggregated under different conditions, whereas usual targets, such as proteins, are more uniform throughout the physiologically relevant range of conditions). For

this we used amyloid-beta peptides aggregated under the markedly different conditions. Probe signature approach gives promises in this direction, but further work is required, since within the limits of the current work it was impossible to achieve conclusive results as to differentiation of “strains”, but we believe that further work based on further elaboration of probe signature and ML can bring results envisioned.

As the feasible additional step which can help to differentiate between the strains on the future stages of this research we suggest conducting disaggregation assay, where after measuring a sample and getting positive results we add a protease specific to the target and measure further RI change. Different aggregates are susceptible to the protease cleavage to different degrees, thus enriching data for the analysis and “strain” differentiation.

4.4 Machine learning and defining unknown concentrations ab initio

Most RI sensors are concerned with detection of presence of the target not its concentration, here we asked if there is possibility to define concentrations of targets as opposed to simple detection. For this we used probe signatures and machine learning approaches.

As of now the results do not allow direct application of this approach but point to an important direction to move if we want to achieve this goal (as well as studies distribution of the target on the probe as already mentioned in section 4.2).

CHAPTER 5 - (CONCLUSION)

The work done showed that several initial goals were achieved, such as validation of usage of biotinylated peptides as BREs for AD as a prion-like disease in case of interferometric fiber optic semi-distributed biosensors which in our knowledge had not yet been described in literature, the same as biotinylating of peptides for more aligned grafting of the BREs on the surface of the probe.

One more idea which was in the basis of this work is that peptides are better than antibodies in detecting presence of pathological aggregates since they bind any nascent oligomer or any other aggregate, whereas antibodies are useful only for a specific epitope. This can be confirmed on the next stage of the research possibly using different antibodies to compare performance between them as well as peptides.

Also, it is imaginable that in case of our modality we can use peptides to detect antibodies in the sample thus giving more flexibility to the procedure.

Another crucial advantage is the size ratio between the BRE and the target: in case of antibodies this ratio is close to 1 or even much less than 1 since antibodies (weight circa 150 kDa) can be used to detect tiny peptides (4,5 kDa in case of Amyloid beta 42). There are of course so called nanobodies (12-15 kDa), but their production is more sophisticated and can be more costly than of traditional ones [37]. We proved that it is feasible to use peptides at least in cases when the investigated condition has explicitly prion nature. Moreover, further work can benefit from assays developed for detection of prions.

There is possibility which was not realized in this work due to the time limits but was visualized and can be done on the later stage of the research enabling further differentiation between the strains of amyloid, namely unbinding assay in which we can measure the rate of dissociation of the target (or even its cleavage by proteases or under the influence of some oxidizing agent), which is particularly

amenable in case of our probes since their performance will not deteriorate in the more extended process of the target unbinding due tot their simple and robust structure requiring minimal amount of preliminary processing. The experiment design and procedure will be the same in all steps except detection where the probe will be incubated with the target (RI measured in the beginning of incubation and after), then detection will proceed the same way as before but this time serial concentrations of a specific protease will be added and change of RI monitored.

Therefore, we believe that this work achieved most of its primary milestones and opened new opportunities to be explored in future.

REFERENCE LIST

[1] D. S. Knopman *et al.*, "Alzheimer disease," *Nat Rev Dis Primers*, vol. 7, no. 1, Dec. 2021, doi: 10.1038/s41572-021-00269-y.

[2] K. P. Kepp, N. K. Robakis, P. F. Høilund-Carlsen, S. L. Sensi, and B. Vissel, "The amyloid cascade hypothesis: an updated critical review," Oct. 01, 2023, *Oxford University Press*. doi: 10.1093/brain/awad159.

[3] L. Makowski, "The Structural Basis of Amyloid Strains in Alzheimer's Disease," May 11, 2020, *American Chemical Society*. doi: 10.1021/acsbiomaterials.9b01302.

[4] H. Zheng and E. H. Koo, "Biology and pathophysiology of the amyloid precursor protein," 2011. doi: 10.1186/1750-1326-6-27.

[5] B. Byrne, E. Stack, N. Gilmartin, and R. O'Kennedy, "Antibody-based sensors: Principles, problems and potential for detection of pathogens and associated toxins," Jun. 2009. doi: 10.3390/s90604407.

[6] C. A. Lane, J. Hardy, and J. M. Schott, "Alzheimer's disease," Jan. 01, 2018, *Blackwell Publishing Ltd*. doi: 10.1111/ene.13439.

[7] "2023 Alzheimer's disease facts and figures," *Alzheimer's and Dementia*, vol. 19, no. 4, pp. 1598–1695, Apr. 2023, doi: 10.1002/alz.13016.

[8] M. Goedert, M. Masuda-Suzukake, and B. Falcon, "Like prions: The propagation of aggregated tau and α-synuclein in neurodegeneration," 2017. doi: 10.1093/brain/aww230.

[9] D. S. Eisenberg and M. R. Sawaya, "Structural Studies of Amyloid Proteins at the Molecular Level," vol. 18, p. 2, 2025, doi: 10.1146/annurev-biochem.

[10] C. Condello and J. Stöehr, "Aβ propagation and strains: Implications for the phenotypic diversity in Alzheimer's disease," Jan. 01, 2018, *Academic Press Inc.* doi: 10.1016/j.nbd.2017.03.014.

[11] J. Chen *et al.*, "Amyloid Precursor Protein: A Regulatory Hub in Alzheimer's Disease," Jan. 01, 2024, *International Society on Aging and Disease*. doi: 10.14336/AD.2023.0308.

[12] Stanley B. Prusiner, "Novel proteinaceous infectious particles cause scrapie," *Science (1979)*, vol. 216, pp. 136–144, Apr. 1982.

[13] J. C. Watts and S. B. Prusiner, "β-amyloid prions and the pathobiology of alzheimer's disease," *Cold Spring Harb Perspect Med*, vol. 8, no. 5, May 2018, doi: 10.1101/cshperspect.a023507.

[14] R. San Gil and A. K. Walker, "Unlocking Disease-Modifying Treatments for TDP-43-Mediated Neurodegeneration," *BioEssays*, Apr. 2025, doi: 10.1002/bies.202400257.

[15] C. S. G. Catumbela and R. Morales, "Transmission of amyloid-β pathology in humans: A perspective on clinical evidence," *Neural Regen Res*, vol. 19, no. 2, pp. 390–392, Feb. 2024, doi: 10.4103/1673-5374.377610.

[16] C. Marcus, E. Mena, and R. M. Subramaniam, "Brain PET in the diagnosis of Alzheimer's disease," Oct. 01, 2014, *Lippincott Williams and Wilkins*. doi: 10.1097/RLU.0000000000000547.

[17] S. Rani *et al.*, "Advanced Overview of Biomarkers and Techniques for Early Diagnosis of Alzheimer's Disease," Aug. 01, 2023, *Springer*. doi: 10.1007/s10571-023-01330-y.

[18] E. Mikuła, "Recent Advancements in Electrochemical Biosensors for Alzheimer's Disease Biomarkers Detection," *Curr Med Chem*, vol. 28, no. 20, pp. 4049–4073, Nov. 2020, doi: 10.2174/0929867327666201111141341.

[19] T. Habeck, S. S. Zurmühl, A. J. Figueira, E. V. S. Maciel, C. M. Gomes, and F. Lermyte, "Cross-Interactions of Aβ Peptides Implicated in Alzheimer's Disease Shape Amyloid Oligomer Structures and Aggregation," *ACS Chem Neurosci*, Dec. 2024, doi: 10.1021/acschemneuro.4c00492.

[20] M. N. S. Karaboğa and M. K. Sezgintürk, "Biosensor approaches on the diagnosis of neurodegenerative diseases: Sensing the past to the future," Feb. 05, 2022, *Elsevier B.V.* doi: 10.1016/j.jpba.2021.114479.

[21] B. H. Lee *et al.*, "Interferometric fiber optic sensors," Mar. 2012. doi: 10.3390/s120302467.

[22] S. Kazhiyev, A. Abdossova, D. Moldabay, A. Rakhimbekova, W. Blanc, and D. Tosi, "Semi-

distributed interferometers fiber-optic sensors for high-sensitivity refractive index detection: Design and sensitivity analysis," *Measurement (Lond)*, vol. 220, Oct. 2023, doi: 10.1016/j.measurement.2023.113327.

[23] G. J. C. Pimentel *et al.*, "Ultradense Electrochemical Chips with Arrays of Nanostructured Microelectrodes to Enable Sensitive Diffusion-Limited Bioassays," 2024, *American Chemical Society*. doi: 10.1021/acsami.4c01159.

[24] M. Antman-Passig *et al.*, "Optical Nanosensor for Intracellular and Intracranial Detection of Amyloid-Beta," *ACS Nano*, vol. 16, no. 5, pp. 7269–7283, May 2022, doi: 10.1021/acsnano.2c00054.

[25] P. Wang, S. Chen, Y. Guan, Y. Li, and A. Jiamali, "An electrochemical sensing platform based on gold nanostars for the detection of Alzheimer's disease marker Aβ oligomers (Aβo)," *Alexandria Engineering Journal*, vol. 81, pp. 1–6, Oct. 2023, doi: 10.1016/j.aej.2023.08.073.

[26] M. Negahdary and H. Heli, "An electrochemical peptide-based biosensor for the Alzheimer biomarker amyloid-β(1–42) using a microporous gold nanostructure," *Microchimica Acta*, vol. 186, no. 12, Dec. 2019, doi: 10.1007/s00604-019-3903-x.

[27] Z. Zhao *et al.*, "Label-free detection of Alzheimer's disease through the ADP3 peptoid recognizing the serum amyloid-beta42 peptide," *Chemical Communications*, vol. 51, no. 4, pp. 718–721, Jan. 2015, doi: 10.1039/c4cc07037b.

[28] M. Novo, S. Freire, and W. Al-Soufi, "Critical aggregation concentration for the formation of early Amyloid-β (1-42) oligomers," *Sci Rep*, vol. 8, no. 1, Dec. 2018, doi: 10.1038/s41598-018-19961-3.

[29] H. Y. Kim *et al.*, "EPPS rescues hippocampus-dependent cognitive deficits in APP/PS1 mice by disaggregation of amyloid-β oligomers and plaques," *Nat Commun*, vol. 6, Dec. 2015, doi: 10.1038/ncomms9997.

[30] B. Zarrilli *et al.*, "Molecular mechanisms at the basis of the protective effect exerted by EPPS on neurodegeneration induced by prefibrillar amyloid oligomers," *Sci Rep*, vol. 14, no. 1, p. 26533, Dec. 2024, doi: 10.1038/s41598-024-77859-9.

[31] Y. Zhao *et al.*, "Detecting and Tracking β-Amyloid Oligomeric Forms and Dynamics In Vitro by a High-Sensitivity Fluorescent-Based Assay," *ACS Chem Neurosci*, 2024, doi: 10.1021/acschemneuro.4c00312.

[32] Y. Dong, X. Zhu, F. Shi, and J. Nie, "Surface photo-anchored PNIPAM crosslinked membrane on glass substrate by covalent bonds," *Appl Surf Sci*, vol. 307, pp. 7–12, Jul. 2014, doi: 10.1016/j.apsusc.2014.02.176.

[33] A. Domaros, D. Zarzeczańska, T. Ossowski, and A. Wcisło, "Controlled Silanization of Transparent Conductive Oxides as a Precursor of Molecular Recognition Systems," *Materials*, vol. 16, no. 1, Jan. 2023, doi: 10.3390/ma16010309.

[34] N. S. K. Gunda, M. Singh, L. Norman, K. Kaur, and S. K. Mitra, "Optimization and characterization of biomolecule immobilization on silicon substrates using (3-aminopropyl)triethoxysilane (APTES) and glutaraldehyde linker," *Appl Surf Sci*, vol. 305, pp. 522–530, Jun. 2014, doi: 10.1016/j.apsusc.2014.03.130.

[35] "Micron Optics ENLIGHT".

[36] P. S. Ganesh, S. Y. Kim, S. Kaya, and R. Salim, "An experimental and theoretical approach to electrochemical sensing of environmentally hazardous dihydroxy benzene isomers at polysorbate modified carbon paste electrode," *Sci Rep*, vol. 12, no. 1, Dec. 2022, doi: 10.1038/s41598-022-06207-6.

[37] G. Bao, M. Tang, J. Zhao, and X. Zhu, "Nanobody: a promising toolkit for molecular imaging and disease therapy," 2021, *Springer Science and Business Media Deutschland GmbH*. doi: 10.1186/s13550-021-00750-5.